An agent-based model to simulate the boosted Sterile Insect Technique for fruit fly management

Esther Gnilane Diouf, Thierry Brévault, Saliou Ndiaye, Emile Faye, Anaïs Chailleux, Paterne Diatta, Cyril Piou

An agent-based model to simulate the boosted Sterile Insect Technique for fruit fly management

Esther Gnilane Diouf[1,2,3], Thierry Brévault[4,5] , Saliou Ndiaye[3], Emile Faye[6], Anaïs Chailleux[6], Paterne Diatta[7], Cyril Piou[1,2]

1. CIRAD, UMR CBGP, F-34398 Montpellier, France
2. CBGP, Univ Montpellier, CIRAD, INRAE, Institut Agro, IRD, Montpellier, France
3. ENSA, Univ Iba Der Thiam, Thiès, Sénégal
4. CIRAD, UPR AIDA, BIOPASS, Centre de recherche ISRA-IRD, Dakar, Sénégal
5. AIDA, Univ Montpellier, CIRAD, F-34398 Montpellier, France
6. CIRAD, UPR HortSys, Univ Montpellier, Montpellier, France
7. ISRA/CRA de Djibélor, Ziguinchor, Sénégal

Abstract

The sterile insect technique (SIT) is a method of biological control of pests and disease vector insects. It includes mass-rearing and release of sterile males of the target species so that wild females mated with sterile males would not produce offspring. An innovative version of this technique, called boosted SIT, relies on the use of sterile males as vectors of biocides to trigger an epizootic in the wild fruit fly population. We built an agent-based model to assess the feasibility of this technique and main modalities of field implementation for the control of the Oriental fruit fly, *Bactrocera dorsalis,* using the entomopathogenic fungi, *Metarizhium anisopliae,* as a biocide. The model, called BOOSTIT (BactrOcera dOrsaliS boosTed sIT), simulates the spatio-temporal population dynamics of fruit flies in three different realistic landscape contexts. The releases of infected and uninfected sterile males were simulated and allowed the transmission of the pathogen within the wild fly population as a result of interactions between individuals. A main output was the measurement of losses in mango production. Validation of the model was done by comparing the simulated population dynamics with data from field monitoring (pheromone traps) in three landscapes of the Niayes area in Senegal. The population dynamics of wild flies were then simulated in an intensive cropping and mono-mango cultivar landscape under three scenarios: (1) without the release of sterile males, (2) with the release of non-contaminated sterile males (SIT) and (3) with the release of

sterile contaminated males (boosted SIT). The results showed that SIT and boosted SIT strongly reduced the density of wild flies and the amount of infested fruit. Although parameters of the pathogen transfer between individuals need to be studied more deeply, results encourage the implementation of field trials to validate the efficacy of boosted SIT to control fruit flies.

Keywords:
Population dynamics; Pattern-oriented modelling; Pest management; Entomovectoring; *Bactrocera dorsalis; Metarhizium anisopliae*

1. Introduction

The Sterile Insect Technique (SIT) is a biological control method that was proposed by Knipling in the 1950s (Klassen et al., 2021). It is defined as a method of pest control using area-wide inundative releases of sterile insects to reduce reproduction in a field population of the same species. SIT represents therefore a type of birth control in which wild female insects do not reproduce when they are inseminated by released sterilized males. In this type of autocidal control, sequential releases of the sterilized insects in adequate sterile to wild male overflooding ratio's lead to a reduction in the pest population. Effective control using sterile males is achieved as part of area-wide integrated pest management (AW-IPM) programs. The SIT was first developed in USA about fifty years ago (Dyck et al., 2021). It is currently applied worldwide and the four strategic options in which sterile insects are being deployed as a component of AW-IPM for insect pest control are suppression, eradication, containment and prevention (Dyck et al., 2021). The SIT has been applied to a number of species of fruit flies, moths, mosquitoes, tsetse flies and screwworm flies.

SIT was first successfully applied to eradicate the New World screwworm, *Cochliomyia hominivorax* (Coquerel, 1958), in 1954 in Curaçao, North America (Baumhover et al., 1955). It has proved successful for the management of fruit flies of economic importance worldwide, including prevention (e.g., *Ceratitis capitata* (Wiedmann,1824) in California, *Anastrepha ludens* (Loew, 1873) in Texas), containment (e.g., *C. capitata* in Guatemala and Mexico), eradication (e.g., *Bactrocera cucurbitae* (Coquillett, 1899) in Japan or *C. capitata* in Chile) or suppression (e.g., *C. capitata* in South Africa, Israel, Spain and Hawaï, *Bactrocera spp*. in Thailand) (Orankanok et al. 2007; Enkerlin, 2021). To improve the efficiency of the SIT, the

entomovectoring technique proposes the use of sterile insects ("entomo") as vectors ("vectoring") of a biocide to one or more targeted life stages of a pest population (Hokkanen and Menzler-Hokkanen, 2007). This is known as boosted SIT (Bouyer and Lefrançois, 2014). Bouyer et al. (2016) used this concept on sterile male mosquitoes coated with pyriproxyfen that contaminate females that can in turn contaminate the larval habitats. This technique has shown its potential in coffee-growing areas in Guatemala where *C. capitata* sterile males, inoculated with *Beauveria bassiana* transmitted spores to 44% of the captured wild males (Flores et al., 2013).

The application of this technique for a given pest in a given area requires knowledge of the life history system of target pests (Lance and McInnis, 2021) to consider how the interactions between individuals and their environment may promote or hinder the boosted SIT. Modelling is a relevant tool as it can generate scenarios that can reduce incertitude and guide field experiments. Many models have been built to answer issues on the effectiveness of SIT. Most focused on release strategies (Cai et al., 2014; Strugarek, 2019), the sterility level of sterile males (Barclay, 1982; Kean et al., 2011), the competitiveness of sterile males and mating preference of females (Vreysen et al., 2006; Chargui et al., 2018), their movement and dispersal, sometimes including the impact of spatial structure of the environment (Tyson et al., 2007; Dufourd and Dumont, 2013). Other studies have looked at the economic cost of SIT (Thomé et al., 2010; Ramirez and Gordillo, 2016) and its combination with other control methods (Barclay and Vreysen, 2011; Douchet et al., 2021). For the boosted SIT, two modelling studies evaluated the feasibility of the approach using pyriproxyfen with *Aedes spp* mosquitoes. Pleydell and Bouyer, (2019) developed a mathematical model to evaluate the gain of the boosted SIT over conventional SIT. They showed that boosted SIT reduced mosquito suppression time and required fewer males to be released. Including environmental conditions in their mathematical model, Haramboure et al., (2020) found that boosted SIT could increase the effectiveness of the SIT when sterile males are not very competitive. Most of the models that we reviewed on both techniques are mathematical population-level models and focus on mosquitoes. Few of them (11%) are generic while only 23% target pests (such as fruit flies, tsetse flies or lepidopterans) rather than mosquitoes.

In the present study, the Oriental fruit fly, *Bactrocera dorsalis* (Hendel, 1912), was selected as a model system. Originally from Asia, *B. dorsalis* was first reported on the African continent in Kenya (Lux et al., 2003), initially thought to be a new species, *B. invadens* (Schutze et al., 2015). After its detection, the pest rapidly spread to several African countries including

Senegal where it was reported in 2004 (Manrakhan et al., 2015). It is highly polyphagous and considerable damages have been observed in mango orchards since its introduction (Rwomushana et al., 2008). Damage is caused when females lay their eggs in the fruit; the larvae feed on it, making the fruit rot and inedible (Badii et al., 2015). These losses have had a great socio-economic impact on people in rural and urban communities involved in the mango value chains across Africa (Wangithi et al., 2021). In addition, the presence of the pest limits farmers' access to export markets as it is classified as an organism under quarantine restrictions by most countries in the world (Clarke, 2005; Badii et al., 2015). This led many producers to apply insecticides that are hazardous to the environment and health of users and consumers (Wangithi et al., 2021). Various control tools have been proposed to growers or tested by research and extension services in Africa: early harvesting, male annihilation technique (MAT), protein bait spot treatments, auto-disseminating of fungal pathogen using traps, mass trapping or the SIT (Sutantawong et al., 2002; Mwatawala et al., 2015; Faye et al., 2016; Wangithi et al., 2021). However, *B. dorsalis* remains a critical issue in fruit and vegetable production in African countries.

The understanding of the population dynamics and dispersal abilities can be very useful to develop appropriate control strategies, including those that are area-wide such as SIT (Hendrichs et al., 2020). Thus the dynamics and the potential distribution of *B. dorsalis* or related fruit flies have been predicted by various populational models. Yonow et al., (2004) presented and simulated with DYMEX a mathematical model describing the population dynamics of *Bactrocera tryoni* (Froggatt, 1897) according to temperature, precipitation and humidity. Stephens et al., (2007) and de Villiers et al., (2015) used CLIMEX to study the effects of climate on the distribution and relative abundance of *B. dorsalis*. They showed that tropical and subtropical climates, except the desert, as well as warm temperate areas, are favorable for *B. dorsalis*. To predict the potential distribution of *B. dorsalis*, Liu et al., (2011), Magagula et al., (2015) and Qin et al., (2019) used the MAXENT software. For the same purpose Gutierrez et al., (2021) used weather-driven physiologically-based demographic models.

The SIT has been tested to control *B. dorsalis* with other monitoring and control methods in Thailand. This study was conducted in pilot programs at the orchard level in Ratchaburi province from 1999 to 2000 (Sutantawong et al., 2002) and from 2000 to 2004 (Orankanok et al., 2007), and in the Phichit province from 2003 to 2004 (Orankanok et al., 2007). From 2008 to 2013, an area-wide integrated pest management (AW-IPM) program using the SIT was implemented in the Chantaburi province (Chinvinijkul et al., 2019). These programs were

effective in controlling the fruit fly and fruit infestations were reduced by at least 50% in all targeted areas. To our knowledge, control programs including boosted SIT have not been yet carried out on *B. dorsalis,* even if the use of entomopathogenic fungi like *Metarhizium anisopliae* ((Metchnikoff) Sorokin, 1883) or *Beauvaria bassiana* ((Balsamo-Crivelli) Vuillemin, 1912) for the control of tephritid is gaining interest in the scientific community. Several studies have explored the use of some *M. anisopliae* isolates for the control of many fruit fly species (Ekesi et al., 2002; Quesada-Moraga et al., 2006, 2008; Dimbi et al., 2009, 2013; Sookar et al., 2014; Onsongo et al., 2019). When the spores of *M. anisopliae* come into contact with the cuticle of the insect, they germinate and penetrate it. If the fungus overcomes the insect's defences, it grows, leads to the death of the insect and then external sporulation follows (Zimmermann, 2007). On *B. dorsalis*, Ouna et al., (2010), Ekesi et al., (2011) and Tora and Azerefegn, (2021) showed that *M. anisopliae* induce high mortality and inoculated sterile or wild fly males could successfully interact with other flies. Thus, they could transfer the fungus to wild fly during mating, mating attempts and male interactions (Novelo-Rincón et al., 2009; Flores et al., 2013; Sookar et al., 2014).

Agent-based modelling has been increasingly used to represent insect pest population dynamics and control techniques (e.g., Manoukis and Colliers, 2021; Manoukis and Hoffman, 2014). The present study presents BOOSTIT (BactrOcera dOrsaliS boosTed sIT), an agent-based model that aims to test the performance of SIT using *B. dorsalis* sterile males coated with the entomopathogenic fungi *Metarhizium anisopliae* when released in mango orchards of the Niayes region of Senegal. To enhance the realism of the model, we based it on the approach of pattern-oriented modelling (POM) that uses real patterns for designing, testing, and parameterizing models. POM attempts to optimize model complexity and reduce uncertainty as it relies on additional data contained in observed patterns. These patterns are defined as a characteristic, clearly identifiable structure in nature itself or in the data extracted from nature. They also provide information on the essential properties of a system. (Grimm et al., 1996; Wiegand et al., 2003; Grimm, 2005; Grimm and Railsback, 2013). POM explicitly refers to spatial and temporal scales and produce comparative predictions that can be tested in the field (Grimm et al., 1996). POM is useful for all types of modelling. In the case of agent-based models (also called individual-based models in ecology (Grimm and Railsback, 2006), patterns can guide model structure by showing what kinds of entities need to be considered and what state variables are needed (Grimm and Railsback, 2013). Using POM for development, the model was designed to integrate strong knowledge on the biology and ecology of *B. dorsalis,*

their dependence on climatic conditions and the phenology of different host plants in the Niayes landscape. The model was evaluated using field data collected over 4 years in the Niayes area. We then compared sterile male release scenarios to study their effect on the *B. dorsalis* population dynamics.

2. Materials and methods

2.1. Model description

The BOOSTIT (BactrOcera dOrsaliS boosTed sIT) model is described according to the Overview, Design concepts, Details (ODD) protocol (Grimm et al., 2020, 2010, 2006) for describing individual- and agent-based models. Implementation was performed using the Netlogo 6.1.1 platform (https://ccl.northwestern.edu/netlogo/6.1.1/). Our source code is freely available on Cirad Dataverse (URL available at the acceptance of paper).

2.1.1. Purpose

BOOSTIT was designed to explore the conditions of effectiveness of boosted SIT (number of released individuals, release date, frequency, site, release pulse) to protect a set of mango orchards by estimating fruit production losses. It simulates the spatio-temporal dynamics of a fruit fly population (here, *Bactrocera dorsalis*), the transmission of a pathogen through fly interactions, the phenology of host plants and the landscape structure of different types of orchards (Fig. 1).

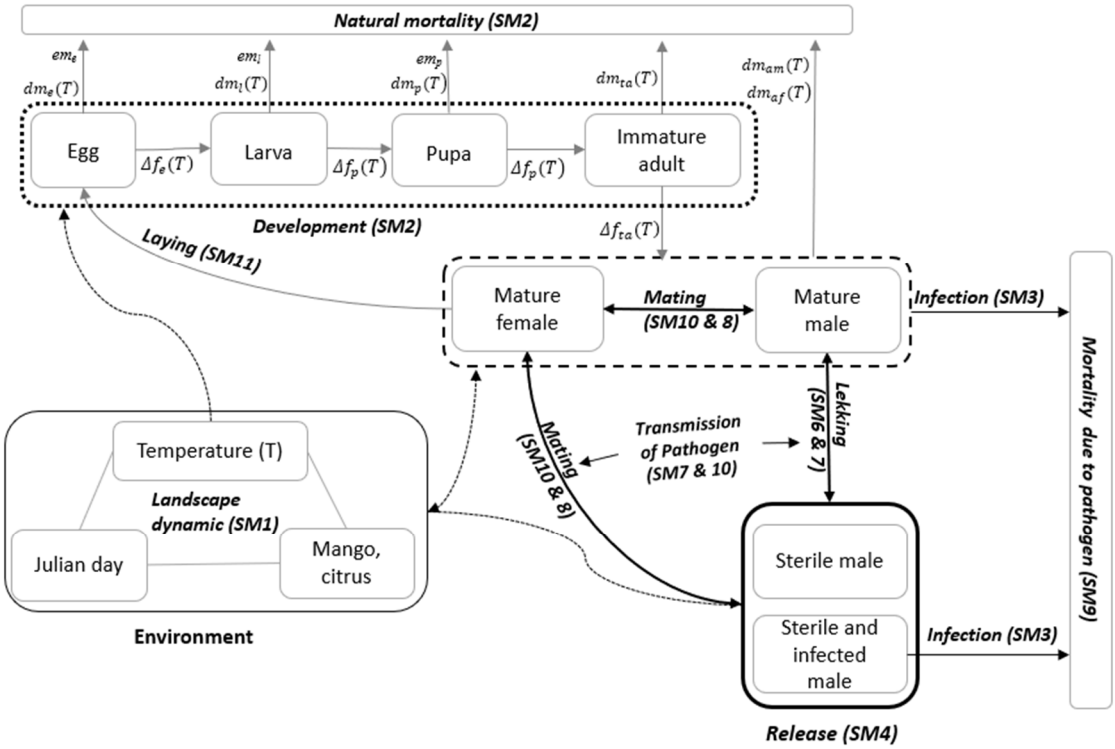

Fig.1. Conceptual diagram of main processes represented in BOOSTIT. Dotted rectangle groups the immature stage of fruit fly life cycle, the rectangle with dash groups the adult stage and the bold rectangle groups the released fly. Grey arrows represent the life cycle. Bold arrows are interactions between flies. Dotted arrows are interactions between flies and the environment. Bold italic shaded texts are processes with *SM* codes corresponding to submodels listed in section *2.1.7.* and table 1. Development functions and mortality probabilities are listed in tables 2 and 3.

2.1.2. Entities, state variables and scales

The model had two entity types: the fly and the spatial unit of landscape that were characterized by state variables.

Landscape cells were described by 8 state variables: the landcover corresponding to habitat types or orchard name, the presence of fruits in the sensitive stage (i.e. mature fruit) (*Frt*), the presence of methyl-eugenol (*Php*), plant type (*Typ*), two counter of the deposited egg number (viable: np_{egg}, total: *Ne*), the carrying capacity of eggs (*Mep*), the counter of days during which they produce fruit at the sensitive stage (*Mtp*).

To characterize flies, 13 state variables were used: the development stage that could be either egg, larva, pupa, immature adult or mature adult, the sex that could be male or female, the development rate (*Dev*), the location, the attractiveness of males (*at*), the mating status of adults (*Mat*), the pre-oviposition time of female (*po*), the number of eggs laid by the female (nf_{egg}), the healthy or infected status, fertility of males (fertile or sterile), the duration of the refractory period between two mating events for females (cp_{mat}), spore number of infected flies (*sp*), and the number of days since the infection (inf_t).

Landscape cells set up the simulation area which comprised four orchards that were separated by a cross of empty cells (Fig. 2). Three types of landscapes of 30.25 ha each with 11 × 11 cells of 2500 m^2 (50 × 50 m) were available: (1) the "*monocultivar landscape*" that formed a landscape of four intensive orchards, (2) the "*low-diversified landscape*" that formed a landscape of two intensive orchards, an extensive orchard and a diversified orchard, (3) the "*high-diversified landscape*" that formed a landscape of one intensive orchard, an extensive orchard and two diversified orchards. Intensive orchards (i.e., intensive cropping system) were considered as monocultivar orchards of high density Kent mango trees. Extensive orchards (i.e., extensive cropping system) were made of different cultivars of mango trees and few citrus trees planted at lower density. Diversified (i.e., diversified cropping system) orchards were

characterized by egual presence of mango trees of different cultivars and citrus trees. These orchard types followed the classification of Grechi et al., (2013). The spatial extent of these orchards (6.25ha) corresponded to realistic Senegalese orchards. In BOOSTIT, they were built with a random spatial distribution of the plant types (*Typ*) from existing proportions of host plants in real orchards from the Niayes area in Senegal (Sarron et al., 2018). We assumed that an average fruit tree covered 25 m² so there were 100 trees per cell. The simulation area was with closed borders (moving flies could not go out of the landscape, the model did not consider emigration nor immigration).

Time was simulated discretely through daily time steps and the horizon of a simulation was a maximum of 1 year (365-time steps). One fly agent in the model was considered to represent 100 flies of the same gender and life stage in the real world. This choice was a good compromise between computation capacities and realism in terms of population structure and size.

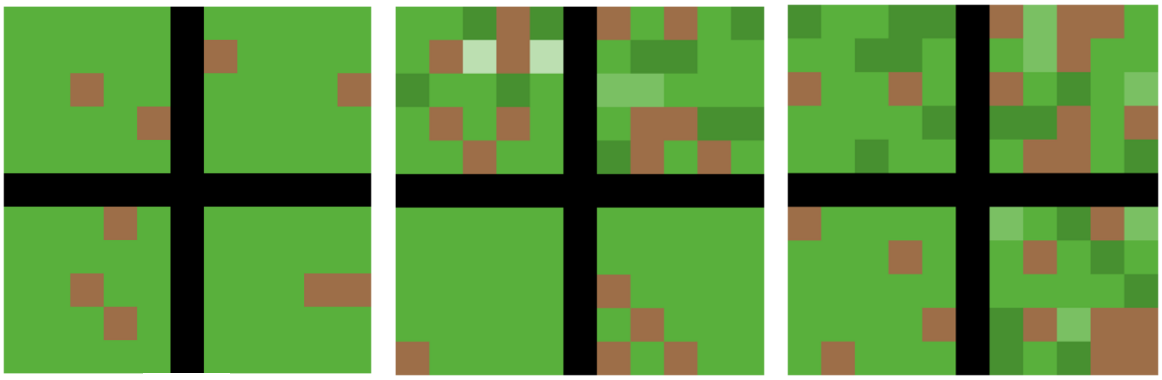

(1) (2) (3)

Fig. 2. Examples of simulation areas from the three types of landscapes: (1) the "*monocultivar landscape*", (2) the "*low-diversified landscape*" and (3) the "*high-diversified landscape*". The cells with dark green are citrus trees, the other different green colour levels represent mango cultivars (see initialization), and the brown cells represent bare soil and shrubs. The black cells are boundary cells that separate four orchards for each simulation area.

2.1.3. Process overview and scheduling

A simulation of the BOOSTIT model began by selecting a type of landscape and by reading a .csv file containing the daily temperature and the ripening period of the fruits of different mango-trees cultivars (see initialization).

At each time step, processes were run in the following order (Table 1): (1) reading input data and calculation of the ripening period of the host plants, (2) the growth and survival processes of the fly, (3) adults that received the minimum dose of infecting spores became infected, (4) the healthy sterile or infected sterile males were released at a chosen date, (5) adults that had not mated had a random movement, (6) lek areas were determined, (7) adult males first increased their attractiveness and then moved to the lek area; if there were males carrying pathogens in leks, they could transmit some of them to some healthy males, (8) some females that had already mated may mate again after a refractory period, (9) some flies died from the infection, (10) a part of female visited the leks in turn and each one chose a male among the most competitive ones and mated with him; if the male carried pathogens, he transmitted some of them to the female. (11) Females that had mated and had passed the preoviposition period laid eggs in cells containing fruit.

For the infection time counter to start on the day after contamination, the processes of releasing sterile and infected males, contamination in leks and contamination during mating came after the infection process. These processes are detailed in section 7 (sub-models).

Table 1.

Scheduling of processes at each time step (= 1 day) of model simulation

Process	Process actor	Submodel
Landscape dynamic	Cell	SM1
Development and mortality	Fly	SM2
Infection	Wild adult female and male	SM3
Sterile male release	Cell	SM4
Random move	Immature and mature fly	SM5
Lek setup	Cell	SM6
Pre-coupling behaviour of males and contamination in lek	Adult male	SM7
Female re-mating	Adult female	SM8
Pathogen mortality	Infected fly	SM9
Partner searching, mating and contamination during mating	Mature adult	SM10
Preoviposition period and laying	Female	SM11

2.1.4. Design concepts

Basic principles

The BOOSTIT model is based on the representation of an epizooty within the population. The individual-fly-centred approach favoured the representation of fine local interactions influencing the life histories of the flies and the transmission of pathogens.

Emergence

Explosive population dynamics emerged from simulated demographic processes at the individual level. The propagation of the disease emerged from inter-individual interactions.

Perception

Male individuals perceived the cells with plants containing methyl-eugenol (*Php*=TRUE) and moved to them to increase their attractiveness, they also perceived potential lek areas (see SM7). Females could perceive leks and cells from a distance equal to their perception radius and on which they could lay eggs (see SM10 & SM11). Females perceived the males but these could not perceive them (see SM10).

Interactions

Interactions were multiple at the inter-individual level and between individual and environmental cells. Males (fertile and sterile) visited cells containing methyl-eugenol to increase their attractiveness and to form lek areas. A female chose a male partner from the most attractive ones before mating. Fertilized females laid their eggs in cells containing ripe fruit. Infected flies could infect other flies during contact in leks or while mating.

Stochasticity

Stochasticity of the model was found both at the initialization and in the dynamics. Initially, adult flies were distributed equitably in the four orchards of the landscape but they positioned themselves on the orchard cells in a random way according to a homogeneous process of spatial Poisson distribution. The fly's survival was a Bernoulli variable; at each stage of life, a fly could either live or die. The selection of the number of flies that died each day or that grew to a higher stage was also a random process (see SM2). The number of females and males visiting the lek areas was determined by a bounded random rate (see SM7 and SM10). The number of females re-mating was randomly selected from those that had already mated (see SM8). If healthy and infected males met in a lek, the selection of healthy males to contaminate was a random process (see SM7); the same applied to the contamination of males and females through mating (see SM10). The mortality of infected adult flies was also a random process (see SM9). The cells of a host plant that would produce mature fruit were chosen randomly. The position of the lek areas on cells with mango trees was random. Unmated adults also had a random movement (see SM5).

Observation

During a simulation of BOOSTIT, the following output variables were monitored graphically on the interface: the number of adult flies, the total number of released sterile or sterile and infected males, the number of infected flies, the quantities of stung fruit per species and per cultivar.

The total quantity of infested mango fruits was calculated by summing the quantities of stung fruit for each cell where eggs were laid. The quantity of stung mango fruits for a cell was calculated by the following equation:

$$sf = (a_{sf} \times \ln(np_{egg}) + b_{sf}) \times \frac{np_{fruit}}{100}$$

where a_{sf} and b_{sf} were parameters (Table 4), np_{egg} was the counter of the viable egg number deposited in the given cell (see SM11), np_{fruit} was a parameter giving a mean number of

mango fruits per cell and per cultivar (Table 4). Here, the number of viable eggs deposited in the cell (see SM10) was used because fruits containing eggs that would not hatch were not considered as damage. In addition, 5 global variables stored the values of the numbers of wild flies and stung fruits at peaks, the dates of these peaks and the annual amount of stung fruit which was the sum of all patches of stung fruit during 365 days.

2.1.5. Initialization

Landscape

At t = 0, the orchard cells had different egg-laying carrying capacities (*Mep*) depending on the type of host plant (*Typ*). It was equal to ac_{kn} for Kent, ac_{ki} for Keitt, ac_{bdh} for BDH, ac_{om} for other mango cultivars and ac_c for citrus (Table 4). To calculate the carrying capacity, we used the maximum number of flies per kilogram of mangoes (130 adults) given by Rwomushana et al. (2008). We supposed that a kilogram of mangoes is composed of two fruits, so we had 65 adults/fruit. Then, the egg-laying carrying capacity per fruit was calculated by adding to the number of adults per fruit the proportion of eggs that did not reach the adult stage (45%) given by Ekesi et al. (2006). To compute the carrying capacity of a cell, we multiplied the carrying capacity of a fruit by the number of fruits per cell np_{fruit} (Table 4). Due to a lack of knowledge on laying preferences, the same carrying capacity was considered for all cultivars of mango trees ($ac_{kn} = ac_{ki} = ac_{bdh} = ac_{om}$). The same computation was done for the carrying capacity of citrus. The methyl-eugenol presence variable (*Php*) was set to TRUE for all cells with mango or citrus trees (see SM7).

Fly

A simulation was typically initialized with the number of adult flies f_{init} (Table 4). Flies were distributed equally in the four orchards with a female/male ratio *fmr* (see Table 4).

2.1.6. Inputs

BOOSTIT took as input a file that contained time series representing the evolution of the following data over a year:

- The date in Julian day,
- The mean daily temperature,
- The ripening period of different mango cultivars and citrus. As infestation increased as fruits ripened (Grechi et al., 2021) this period was considered the mango ripening period (ripe and over-ripened stages). These different fruits were grouped under the following

categories: the mango cultivars Kent, Keitt, BDH (bouko diekhal), the other mango trees and the citrus.

The daily temperature came from the average of three years of data of a weather station (Hobo U30, Onset corp., USA equipped with a temperature and relative humidity S-THB-M002 sensor) located in Sangalkam, in the Niayes area of Senegal (14° 47.338'N, 17° 13.602'W). The mango ripening periods were extracted from work carried out in the same area. These corresponded to probabilities for each cultivar to become mature during the year.

2.1.7. Submodels

The model included 11 sub-models described below and referenced with their procedure names found in Table 1.

2.1.7.1. Landscape dynamic SM1

Reading input data

For a given host plant type, when the time of its fruit maturity (given by the input data file) arrived, the proportion of cells of this plant type that would produce mature fruits (*Frt* = TRUE) was given by a rate chosen in the range of 0 to p_m following a uniform distribution. Considering that cells that already had mature fruit in the year could not produce mature fruit again, the upper limit p_m was calculated by:

$$p_m = ((p_{acc} \times np_v) - np_{vm}) / np_v$$

with p_{acc}, the probability of daily maturity given by the input file for the fruit cultivar considered, np_v the number of cells of the given host plant and np_{vm} the number of cells of the same host plant which fruits were already mature.

Once fruits were available, the counters of the deposited egg np_{egg} and the ripening period (Sensibility to fruit flies) of the fruit *Mtp* were at 0. The duration of host plant maturity depended on the type of plant (Ndiaye 2009). We had ml_{kn} for the Kent, ml_{ki} for the Keitt, ml_b for the BDH, ml_o for the other mango cultivars and ml_c for citrus (Table 4). At the end of the maturity period (given by the csv file), the counter of the deposited eggs np_{egg} became equal to the carrying capacity of the cell (see initialization).

Calculation of fruits maturity time

The *Mtp* counter was incremented for the cell containing ripe and over ripened fruit and during this period, females could lay their eggs in the cell. When the counter reached the ripening time

364 ml_{kn} or ml_{ki} or ml_{bdh} or ml_{om} or ml_c (Table 4), we supposed that the trees had lost their fruits (*Frt*
365 = FALSE). So, no more eggs could be laid in that cell until the following year.

366 *2.1.7.2. Life cycle SM2*

367 *Development*

368 The fruit fly had 5 developmental stages: egg, larva, pupa, immature adult, mature adult (García
369 Adeva et al., 2012). Each individual of the immature stage had a daily development rate (Δf)
370 and a cumulative development level (*Dev*) that allowed it to move on to the next stage. At each
371 time step, the model calculated for each individual, its daily development rate (Δf) based on
372 daily temperature (Table 2). This Δf was then incrementing the variable *Dev*
373 ($Dev_{t+1} = \Delta f + Dev_t$) and when *Dev* was greater than or equal to 1, the fly moved on to the
374 next stage.

375

376 **Table 2**

377 Development rates of the different fly life cycle stages (García Adeva et al., 2012). In these equations, T represent
378 the temperature (Illustration Appendix A)

Stage	Δf
Egg	$\Delta f_e(T) = \begin{cases} a_{de} \times min(T, 37) - b_{de} \; if \;\; T \geq 12 \\ 0 \;\; if \; T < 12 \end{cases}$
Larva	$\Delta f_l(T) = \begin{cases} a_{dl} \times T - b_{dl} \; if \;\; T \geq 10 \\ 0 \; if \; T < 10 \end{cases}$
Pupa	$\Delta f_p(T) = \begin{cases} a_{dp} \times T - b_{dp} \; if \;\; T \geq 12 \\ 0 \; if \; T < 12 \end{cases}$
Immature adult	$\Delta f_{ta}(T) = \begin{cases} a_{dia} \times T - b_{dia} \; if \;\; T \geq 12 \\ 0 \; if \; T < 12 \end{cases}$
Mature adult	*0*

379

380 *Mortality*

381 The model included two types of fly mortality. The establishment mortality *em* applied to the
382 immature stages of the fly when they entered a given stage and the daily mortality *dm* which
383 varied with temperature *T* (Table 3) and was applied to all stages at each time step. These

mortality events were simulated using a random selection based on a uniform distribution in intervals from 0 to *em* and 0 to *dm* respectively.

Table 3

Mortality probabilities per moult (*em*) and per day (*dm*) for different stages of the life cycle. In these equations, *T* represents temperature (Figure in Appendix B). Values of parameters are given in Table 4.

Stage	Establishment mortality	Daily mortality	References
Egg	em_e	$dm_e(T) = \begin{cases} -a1_{me} \times T + b1_{me} \; if \;\; T < 2 \\ a2_{me} \times T - b2_{me} \; if \; T > 32 \\ 0 \; if \; 2 \leq T \leq 032 \end{cases}$	em_e (Yonow et al., 2004) dm_e (García Adeva et al., 2012)
Larva	em_l	$dm_l(T) = 1 - (a_{ml} \times T^2 - b_{ml} \times T + c_{ml})$	em_l (Ekesi et al., 2006) dm_l (García Adeva et al., 2012)
Pupa	em_p	$dm_p(T) = \begin{cases} a1_{mp} \times T + b1_{mp} \; if \;\; T < 5 \\ a2_{mp} \times T - b2_{mp} \; if \; T > 31 \\ 0 \; if \; 5 \leq T \leq 31 \end{cases}$	em_p (Ekesi et al., 2006) dm_p (García Adeva et al., 2012)
Immature adult	*0*	$dm_{ta}(T) = \begin{cases} -a1_{mia} \times T - b1_{mia} \; if \;\; T < -2 \\ a2_{mia} \times T - b2_{mia} \; if \; T > 36 \\ 0 \; if \; -2 \leq T \leq 36 \end{cases}$	García Adeva et al., 2012
Mature male adult	*0*	$dm_{am}(T) = 1 - 0.5^{e\,(a_{mm} \times T - b_{mm})}$	Adjusted from the survival function and the expectation data given in Yang et al., 1994
Mature female adult	*0*	$dm_{af}(T) = 1 - 0.5^{e\,(a_{mf} \times T - b_{mf})}$	Adjusted from the survival function and the expectation data given in Yang et al., 1994

2.1.7.3. B. dorsalis infection SM3

Flies carrying pathogens became infected if their number of spores *Sp* was greater than the minimum number of spores required to cause the death of the fly sp_{min} (Table 4). The counter of days of infected fly inf_t was incremented from the time-step following infection.

2.1.7.4. Sterile male release SM4

When the simulation day corresponded to the first release day chosen rm_t (Table 4), sterile adult males were released. These males were released by cells chosen either at the centre or at four points in the 4 orchards of the landscape. They had at that moment the maximum degree of

attractiveness $at_{sm} = at_{max}$ (Table 4). This supposes that sterile males were fed with methyl-eugenol before their release to make them equally or more competitive than wild males (Orankanok et al., 2013). They were either healthy, meaning that they did not carry the pathogen, or infected, meaning that they carried the pathogen. The number of sterile males to be released rm_{nb} was calculated by:

$$rm_{nb} = wm_t \times r_{sw}$$

where wm_t was the number of wild males present in the landscape at the release time, r_{sw} was the ratio of sterile males by wild males desired for release (Table 4). The maximum number of sterile males to be released was rm_{max} and the minimum was rm_{min} (Table 4); these limits were added to avoid the release of too few or too many sterile males making the model outputs unrealistic. Two release modalities were possible for a landscape. On the one hand, for the *one-zone* option, the number of sterile males was divided by 4 and then the cell in the centre of each orchard of the landscape released $^1/_4$ of the number of sterile males. On the other hand, for the *multi-zone* option, the number of sterile males was divided by 16 and four cells of each orchard of the landscape were picked to release each $^1/_{16}$ from the number of sterile males. The number of releases was defined as nb_{rel} and the time interval between releases as int_{rel} (Table 4).

For sterile and infected males, the number of spores on each of them followed a normal distribution with a mean sm_{sp} and standard deviation sd_{sp} (Table 4).

2.1.7.5. Random move SM5

Although *B. dorsalis* can fly for many kilometres, we assume that it can also restrict its movements in a favourable environment (Fletcher, 1987). For this study, long-distance fly migrations were not included in the simulated landscape. To simulate the dispersion ability of *B. dorsalis*, this submodel of random move is called for all adult (immature or mature) flies that were not mating the previous time step. These flies were set to follow a random movement in the orchard. They turn left or right between 0 and 180 degrees and then move forward for 50 m. This random move led some flies to cross the boundary cells (separating the orchards) of the landscape but could not go out of the landscape.

2.1.7.6. Lek setup SM6

At each time step, the number of lek areas n_{lek} was calculated from the number of adult males n_{am} that were present in the orchard:

$$n_{lek} = n_{am}/mean_{mlek}$$

Where $mean_{mlek}$ (Table 4) was an observed mean number of males per lek (Ekanayake et al., 2017). The lek areas could be located on any potential cells located in the orchard and containing mango trees or citrus trees. The lek areas were not fixed, they changed at each time step.

2.1.7.7. Pre-coupling behaviour of males and contamination in lek SM7

Before mating, adult males (sterile or not) that entered a cell with methyl-eugenol increased their attractiveness of a rate inc_{at} (Table 4). This was based on the fact that plant products containing methyl-eugenol ingested by males are incorporated into their sex pheromone, making them more attractive to female flies (Clarke, 2005). Any adult male in the model could visit the nearest lek area to mate. The proportion of male rm_{lek} (Table 4) visiting lek each day was the result of random selection for each male following a uniform distribution over an interval from 0 to rm_{lek}. If a male took part in the courtship in the leks, it released a part lek_{at} (Table 4) of its attractiveness. Otherwise, it continued to increase its attractiveness up to the maximum at_{max} (Table 4).

If there were infected males in a lek, they could transmit spores to a randomly chosen number of males according to a uniform distribution with a probability between zero and tr_c (Table 4). The number of spores collected by the recipient male was calculated by:

$$sp_r = sp_c \times sp_d$$

Where sp_c was the proportion of spores transmitted during male interactions in leks and sp_d was the number of spores from the donor male (Table 4). The remaining number of spores from the donor male was thus calculated by:

$$nsp_d = sp_d - sp_r$$

2.1.7.8. Female re-mating SM8

Female polyandry is common in fruit flies (Shelly, 2000). In BOOSTIT, a portion of adult females among those that had already mated would re-mate after a refractory period p_{mat} (Table 4). The cp_{mat} counter first incremented for females for which it was positive (SM10) and, when it became equal to the refractory period p_{mat}, the female had a probability r_{mate} (Table 4) to re-mate simulated through the comparison of a random number following a uniform distribution ranging from 0 to 1 and r_{mate} (Table 4). The cp_{mat} counter was then reset to zero for these females.

2.1.7.9. *Pathogen mortality SM9*

Adult females and males with spores and who had received sufficient spores to cause its lethality became infected. When the infection time counter inf_t (see SM3) became greater than or equal to the chosen incubation period t_{incub} (Table 4), the infected flies had a probability to die f_{mort} for females and m_{mort} for males (Table 4). These flies were then removed from the simulation.

2.1.7.10. *Partner searching, mating and contamination during mating SM10*

A proportion of adult female f_{mate} (Table 4) that was not mated (*Mat* = FALSE) or that had exceeded the refractory period after a first mating were set to go to the nearest lek area. Each female chose and mated with one of the most competitive unmated males i.e the ones who had released the most pheromone lek_{at} (SM8). The female immediately became mated (*Mat* = TRUE) and the cp_{mat} counter became equal to 1. If the selected male was sterile, the $mat_{sterile}$ counter incremented and if it was fertile the mat_{wild} counter incremented. These counters respectively measured the number of mattings with sterile males and the number of mattings with wild males. If the male was contaminated, there was a probability *trf* (Table 4), that the female became also contaminated. In that case, the number of spores transmitted to the female by the donor male was calculated by:

$$sp_f = sp_m \times sp_d$$

where sp_m was the percentage of spores transmitted during mating and sp_d was the number of spores of the donor male (Table 4). The male became mated (*Mat* = TRUE) and its residual spore number became:

$$nsp_d = sp_d - sp_f$$

2.1.7.11. *Preoviposition period and laying SM11*

A female that had just emerged had a pre-oviposition period *po* (in days) computed by the following function:

$$po = a_{po} \times T^2 - b_{po} \times T + c_{po}$$

where T was the daily temperature, a_{po}, b_{po} and c_{po} were parameters (Table 4), (Yang et al., 1994), (Illustration Appendix C). The po_c counter incremented once the female reaches the immature adult stage and continued when it became an adult. During the pre-oviposition period, the female could not lay eggs even if it was mated. When $po_c >= po$ then the female became able to lay and the poc counter was set to the po value.

The female that had already mated, had exceeded the pre-oviposition period and had not yet laid the maximum number of eggs $fmax_{egg}$ (Table 4) that it could lay, was searching for cells containing mature fruit (see SM1), located in its perception radius *pr* (Table 4). If the cell had not reached its carrying capacity (*Ne*<*Mep*, cf initialization), the female laid the number of eggs calculated by:

$$tolay = -a_{lay} \times T^2 + b_{lay} \times T - c_{lay}$$

where *T* was the daily temperature, a_{lay}, b_{lay} and c_{lay} were parameters (Table 4) (Yang et al., 1994) (Illustration Appendix D). Since the female would lay non-viable eggs if it mated with a sterile male, the number of eggs that would hatch would depend on the number of times the female had mated with a wild male or with a sterile male. The number of eggs that would hatch was computed as:

$$tolay_{final} = tolay \times mat_{wild} \div (mat_{wild} + mat_{sterile})$$

where mat_{wild} and $mat_{sterile}$ were counters (see SM10).

The number of eggs laid by a female nf_{egg} was the sum of the numbers of viable and non-viable eggs. The number of eggs deposited on the cells np_{egg} was considered to be the sum of the viable egg only.

Table 4

BOOSTIT parameter descriptions and selected values

Parameter	Value	Description	Intervention step	References / comments
		Fly		
f_{init}	200	Initial fly number for a landscape of 100×100-cell and 10×10-cell respectively	Initialization	Adjusted after simulations (see discussion)
r_{fm}	1:1	Ratio female/male	Initialization	(Yonow et al., 2004)
a_{de}, b_{de}	0.0382, 0.4229	Parameters of egg development parameters	SM2	(García Adeva et al., 2012)
a_{dl}, b_{dl}	0.0061, 0.0609	Parameters of larval development parameters	SM2	(García Adeva et al., 2012)
a_{dp}, b_{dp}	0.0061, 0.068	Parameters of pupal development parameters	SM2	(García Adeva et al., 2012)
a_{dia}, b_{dia}	0.0108, 0.133	Parameters of immature adult's development parameters	SM2	(García Adeva et al., 2012)

em_e	0.09	Parameters of egg establishment mortality	SM2	(Yonow et al., 2004)
em_l	0.24	Parameters of larval establishment mortality	SM2	(Ekesi et al., 2006)
em_p	0.19	Parameters of pupal establishment mortality	SM2	(Ekesi et al., 2006)
$a1_{me}$, $b1_{me}$, $a2_{me}$, $b2_{me}$	0.0729, 0.1354, 0.1706, 5.4585	Parameters of egg daily mortality	SM2	(García Adeva et al., 2012)
a_{ml} , b_{ml} , c_{ml}	0.0003, 0.0105, 0.1146	Parameters of larval daily mortality	SM2	(García Adeva et al., 2012)
$a1_{mp}$, $b1_{mp}$, $a2_{mp}$, $b2_{mp}$,	0.025, 0.125, 0.0457, 1.4192	Parameters of pupal daily mortality	SM2	(García Adeva et al., 2012)
$a1_{mia}$, $b1_{mia}$, $a2_{mia}$, $b2_{mia}$	0.07, 0.13, 2 0.125, 4.5	Parameters of immature adult daily mortality	SM2	(García Adeva et al., 2012)
a_{mm}, b_{mm}	0.0835, 6.0040	Parameters of mature male daily mortality	SM2	(Yang et al., 1994)
a_{mf} , b_{mf}	0.0782, 5.7669	Parameters of mature female daily mortality	SM2	(Yang et al., 1994)
a_{po} , b_{po}, c_{po}	0.2385, 14.165, 221.93	Parameters of the pre-oviposition period of the female	SM2	(Yang et al., 1994)
a_{lay} , b_{lay} , c_{lay}	0.08, 4.17, 48.60	Parameters of egg-laying of the female	SM11	(Yang et al., 1994)
$mean_{mlek}$	10	Mean male number in a lek	SM6	(Ekanayake et al., 2017)
p_{mat}	20.5	Mean day number during which a female doesn't mate after a first mating	SM8 and SM10	(Wei et al., 2015)
f_{mate}	0.30	The proportion of females that mate every time step	SM10	(Clarke et al., 2005)
p_{mat}	20.5	Mean day number during which a female doesn't mate after a first mating	SM8 and SM10	(Wei et al., 2015)
pr	3	Perception radius of fruit by the female for respectively 100×100-cell and 10×10-cell landscape	SM11	-
$fmax_{egg}$	1428	The maximum egg-laying capacity of female	SM11	(Ekesi et al.,2006)
		Sterile male release and pathogen contamination		
rm_t	153	Start date of sterile male release	SM4	Adjusted after exploration
r_{sw}	5:1	Sterile male / wild male ratio	SM4	Adjusted after exploration
nb_{rel}	10	Release number of sterile males	SM4	Adjusted after exploration

int_{rel}	7	Interval of sterile male release	SM4	Adjusted after exploration
rm_{max}	10000	Maximum threshold of sterile male that can be released	SM4	Threshold added to avoid having too many males to be released
rm_{min}	100	Minimum threshold of sterile males that can be released	SM4	Threshold added to avoid having too few males to be released
at_{sm}	100	Attractiveness of sterile male	SM4	
sm_{sp}	414285	Initial mean spore number of sterile males	SM4	Unpublished data
sd_{sp}	419783	Standard deviation of initial mean spore number of sterile males	SM4	Unpublished data
t_{incub}	2	Incubation time of an infected fly	SM9	Unpublished data
tr_f	0.34	Pathogen transmission rate during mating	SM10	Unpublished data
tr_c	0.34	Contact transmission rate	SM7	Adjusted to transmission rate during mating
sp_m	0.3	Proportion of spores transmitted to female during mating	SM10	Unpublished data
Sp_c	0.5	Proportion of spores transmitted to male during the lek	SM7	Unpublished data
sp_{min}	300	Minimum spore number that can infect the fly	SM3	-
f_{mort}	0.0235	Lethality rate of infected female	SM9	Unpublished data
m_{mort}	0.05	Lethality rate of infected male	SM9	Unpublished data
		Landscape		
a_{sf} , b_{sf}	14.438, 9.1275	Stung fruit parameter	Initialization	(Ekesi et al., 2006; Rwomushana et al., 2008)
ac_{kn}	180	Kent carrying capacity	Initialization	Calculated with Rwomushana et al., (2008) data
ac_{ki}	180	Keitt carrying capacity	Initialization	Calculated with Rwomushana et al., (2008) data
ac_{bdh}	180	BDH carrying capacity	Initialization	Calculated with Rwomushana et al., (2008) data
ac_{om}	180	Other mango carrying capacity	Initialization	Calculated with Rwomushana et al., (2008) data
ac_c	11	Citrus carrying capacity	Initialization	Calculated with Rwomushana et al., (2008) data

ml_{kn}	7	Kent sensitive period to egg-laying	SM1	Shorter than ml_{ki} because Kent mango were collected early for exportation
ml_{ki}	30	Keitt sensitive period to egg-laying	SM1	Corresponds to the mango ripening and over ripened period
ml_{bdh}	30	BDH sensitive period to egg-laying	SM1	As ml_{ki}
ml_{om}	30	Other mango sensitive period to egg-laying	SM1	As ml_{ki}
ml_{c}	30	Citrus sensitive period	SM1	Corresponds to a general duration of maturation of citrus fruits
np_{fruit}	15200	Mean fruit number per patch (number of fruits per mango tree (152) times the number of trees per patch (100))	Observation	unpublished data

2.2. Simulations

2.2.1. Validation experiment

The data for validation came from three studied orchards located in the Niayes area of Senegal. For each orchard, the host plant composition of surrounding orchards (recorded in a database of orchard monitored in the Niayes area in 2011), within a radius of 275m around the centre, was considered to define the landscape cropping system type to which the orchards belong. The mango cultivars and other tree species of each of these landscapes matched with the composition of a BOOSTIT landscape: an intensive landscape with only Kent cultivar, a low-diversified landscape with mainly Kent, some other mango cultivars, citrus and other tree and a high-diversified landscape with many mango cultivars, citrus and other trees. The *B. dorsalis* males captured with methyl-eugenol traps were recorded weekly from January 2011 to December 2014 in the three chosen orchards. The high-diversified orchard had 2 traps, the two others had three traps. We first computed the mean daily number of trapped males per trap for each orchard. Then, we computed the relative proportions of the number of males captured to the maximum number of annual captured males during each of the four years. A running average over a 7 days window was computed across the 4 years of data to have a mean, minimum and maximum relative number of captured flies per Julian day. The BOOSTIT simulations were done on 365 Julian days from January the 1st for the three landscapes. Each run was replicated 100 times with input data as described in section 2.1.6 and parameters in table 4. We assume that the traps capture a proportion of the males present in the real orchards.

These data cannot be directly compared to the fly data simulated by the model. To make a comparison, the relative proportions to the maximum number of annual males in each of the two cases (captured and simulated) were used. To validate our model, we focused on the reproduction of four aspects of the time series: (1) the sharp increase of population size at a given date; (2) the timing of the maximum population size (peak); (3) the decrease rate of the population after the peak; (4) the differences between the three landscapes.

2.2.2. Scenarios of sterile flies' release

To examine the effect of SIT and boosted SIT on the fly population dynamics and the infested fruit abundance, we simulated three scenarios with the intensive landscape: (1) a scenario of the fly population dynamics according to the resource availability and the daily temperature without management implementation; (2) a scenario of the fly population dynamics under effects of SIT; (3) a scenario of the fly population dynamics under effects of boosted SIT. We chose the intensive landscape because for this paper we did not focus on the effect of the different landscapes on SIT and boosted SIT. Preliminary exploration of the parameters related to the release of sterile males allowed to choose a combination of values of these parameters that showed an effect of both SIT and boosted SIT on the amount of stung fruit. The first release of sterile males was on day 153 (rm_t, Table 4) which corresponds to the beginning of June. Ten releases were done in total at an interval of 7 days (nb_{rel} and int_{rel}, Table 4). Males were released at the centre of each of the four orchards with a ratio sterile/wild of 5/1 (r_{sw}, Table 4). We simulated the model with selected parameters following Table 4 from January the 1st over 365 Julian days. For each simulation, we made 100 replicates. The mature wild adult number at each time step and the annual amount of fruit were recorded. Then we calculated the annual mean of the 50 replications for each output. To obtain density per square meter measures, the mean numbers of wild adult fly was first multiplied by the aggregation unit 100 and divided by the real area of the simulation landscape (see section 2.1.2.).

3. Results

3.1. Model validation

The dynamics of simulated males was close to that of males captured in Niayes orchards (Fig. 2). The simulated fly abundance was related to the host plant availability. On day 160 when no mature mango of the Kent cultivar occurs yet, the simulated mean males' number for the landscapes (a), (b) and (c) respectively, were 1300, 3000 and 3700. This presence of flies more pronounced in landscapes (b) and (c) was due to the abundance of alternative host plants that enabled flies to reproduce until the sensitive period of the Kent cultivar. This is why there was

562 a faster increase in the number of simulated males in landscapes (b) and (c) than in landscape
563 (a). This trend was also observed on field data with peaks occurring earlier on days 209 and
564 210 for (b) and (c) and later on days 223 for (a). In simulations, the peak occurred around the
565 226th day for the three landscapes. The predominance of Kent in landscapes compared to other
566 host plants strongly influenced the abundance of the flies. Hence, the model successfully
567 reproduced the sharp increase of population size for the three landscapes. The timing of the
568 population peak was well reproduced for landscape (a) but was not as good for the two other
569 landscapes. The decrease rate of the population after the peak was slower in the simulation than
570 what was observed in the field.

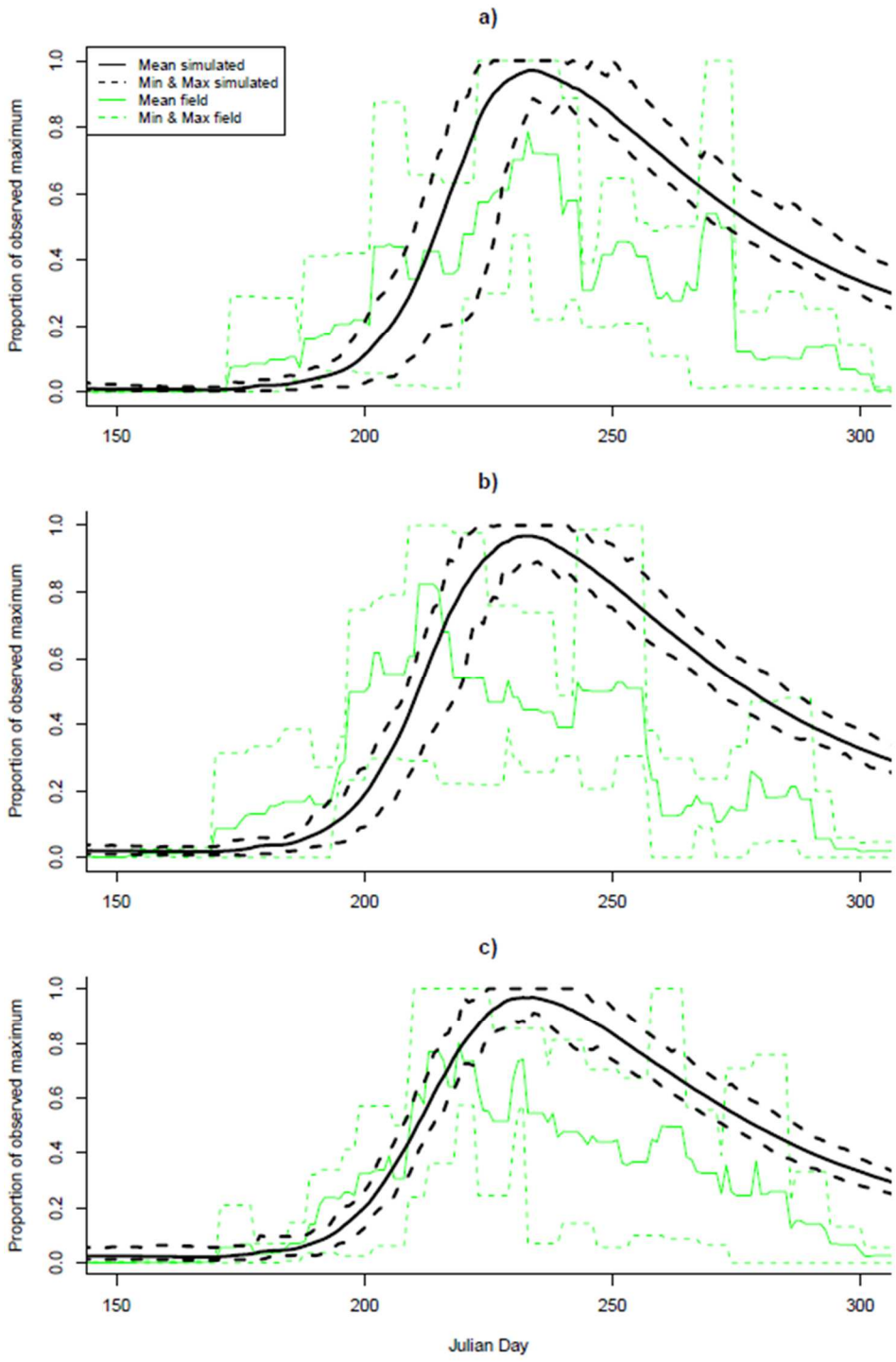

571

572 **Fig. 3**: BOOSTIT validation. Comparison of the dynamics of males collected in three landscape
573 types located in the Niayes area from 2011 to 2014 (*green lines*) with dynamics of males
574 simulated in BOOSTIT (*black lines*). (a) monocultivar landscape, (b) low-diversified
575 landscape, (c) high-diversified landscape. The number of real and simulated males were
576 expressed as relative proportions to their maximum number of annual males. Solid lines are the
577 average proportions of male number and dotted lines represent the minimum and the maximum
578 proportion of males.

3.2. *Scenario simulations*

3.2.1. *Reduction of fly abundance*

The exploration of fly abundance per square meter in the unmanaged scenario showed an important variation of mean values with a peak around the 234th Julian day (Fig. 4). As expected, we observed a decrease in the density of flies when sterile males were released, with a greater effect of boosted SIT. The mean peaks for the SIT and boosted SIT scenarios occurred on day 244. Both techniques succeeded in delaying the fly peak by 10 days. These delays were caused by the slower growth of populations under SIT and boosted SIT also limited by the beginning of the decrease of fruit availability. After these peaks, the number of flies decreased until the end of the year in all three scenarios as the resources for egg-laying decreased. We observed a faster decrease of wild adults in the case of boosted SIT than in SIT. This was caused by mortality resulting from the contamination of wild adults by infected sterile males.

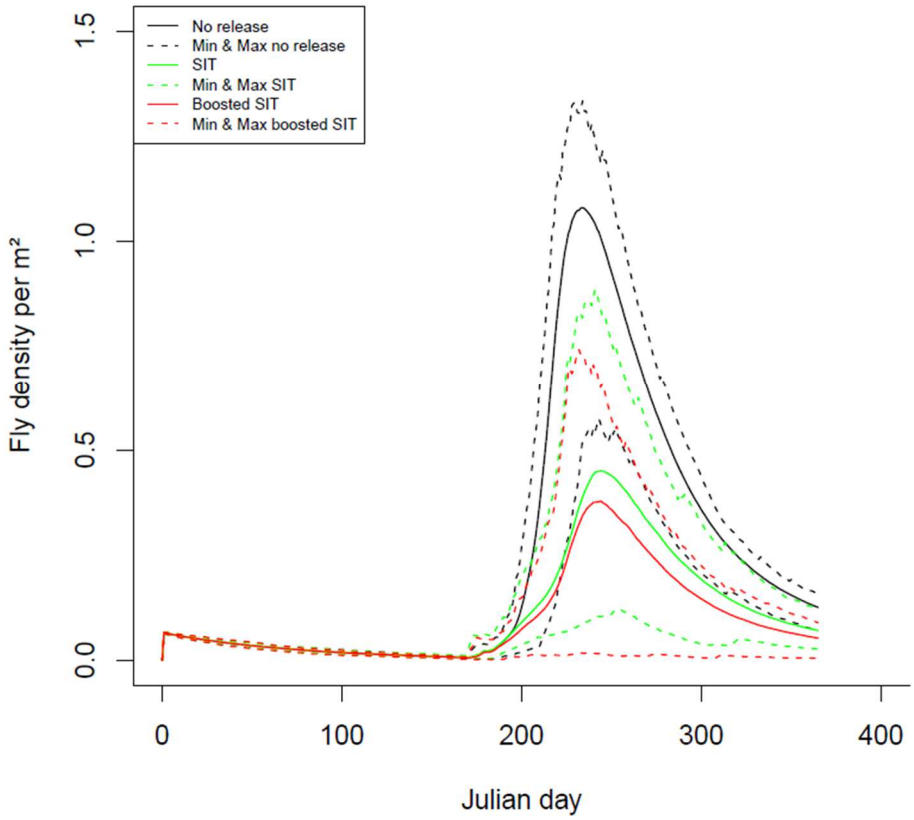

Fig. 4: Fly abundance per square meter for three simulated scenarios for the intensive landscape. Non-release of males (*black lines*), release of sterile and non-infected males (*green lines*), and release of sterile infected males (*red lines*). Solid lines are the mean and dotted lines represent the minimum and maximum of the 50 simulations.

3.2.2. *Reduction of stung fruit*

The amount of infested fruit was summarized at three Julian dates (Table 5). These dates were chosen to refer to the end of harvesting in the Niayes area for the exportation market (July 16th), the peak of adult flies when sterile males were released (September 1st) and the end of a simulation year (December 31st). The amount of infested fruits was reduced by about 30% when sterile (contaminated or not) males were released for all three dates (Table 5). The number of females was therefore reduced with both control methods. Boosted SIT reduced the average and minimum values of stung fruits compared to the SIT. However, the boosted SIT sometimes increased the variability of outputs with higher maximums at the 197th and 244th days than SIT. This originated from additional random processes of contamination and mortality due to the pathogen.

Table 5. Average, minimum and maximum quantity of infested fruits for the three scenarios at three dates: July the 16th (197), September the 1st (244) and December the 31st (365).

	Average			***Minimum***			***Maximum***		
Julian day	***197***	***244***	***365***	***197***	***244***	***365***	***197***	***244***	***365***
No release	368 551	980 986	1 013 939	110 957	659 622	683 941	450 705	1 098 113	1 122 432
Sterile insect release	214 756	687 801	720 306	110 419	433 151	469 630	326 095	935 356	971 835
Boosted SIT	209 727	684 883	712 399	49 418	164 012	186 983	344 344	944 487	968 807

The gain in the reduction of the number of flies with boosted SIT seen in the previous section was largely reflected in the amount of stung fruit. However, in some simulations, boosted SIT was not successful because pathogen transmission was very low and mortality of sterile males was very high. The fly population exploded and reached the peak more quickly than in the SIT simulations (see the maximum curve in Fig. 4). In the SIT scenario, the mortality of sterile males was very low so even if control was not entirely successful, it could delay the peak compared to boosted SIT. When the peak was delayed, the number of stung fruits was lower than when the peak occured early (Fig. 5). Hence, the quantity of stung fruits in the boosted SIT scenario was higher than in the SIT scenario.

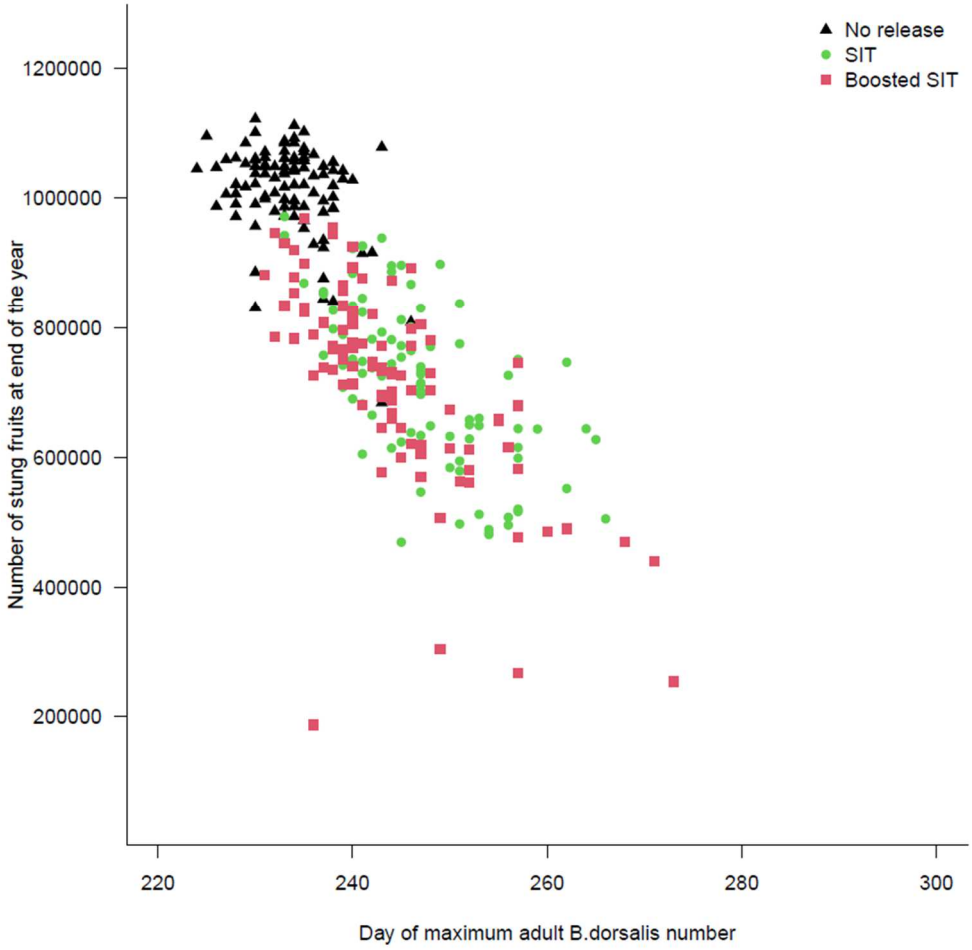

620

621 **Fig. 5**: Relationship between the number of stung fruits at the end of a simulation year and
622 the dates of the peak of adult number.

623 **4. Discussion**

624 We developed the agent-based model BOOSTIT to simulate the spatial and temporal dynamics
625 of populations of the oriental fruit fly in heterogeneous landscapes under the influence of
626 resource availability and releases of sterile males. The simulated dynamics of fruit flies was
627 consistent with that observed in the field. Then, we compared three scenarios in the
628 monocultivar landscape : no release of sterile males, release of sterile males and release of
629 sterile and contaminated males. Results showed that SIT and boosted SIT can significantly
630 reduce the abundance of flies in orchards, especially with the boosted SIT option. We also
631 observed a decrease in the amount of infested fruits but with high variability between
632 simulations of the boosted SIT scenario.

633 The BOOSTIT model allowed an in-depth representation of interactions between flies and with
634 their environment, as the success of the pathogen transmission relied on them. We used time-
635 series of daily temperature and maturity probability of the mango cultivars and citrus measured

636 in the Niayes area. The maps used to build landscapes were simplified from three orchards
637 mapped in the same area with realistic and various host tree spatial distributions and
638 composition. An interesting aspect of our POM approach is that we used spatial and temporal
639 information to design our model but only temporal information for validation. Adjusting
640 complex agent-based models on time series is challenging (e.g., Wiegand et al., 1998; Piou and
641 Prévost 2012). However, in our case, the population dynamics following field data emerge from
642 the interactions between individual fly and the fruit resource phenology. Relying on observed
643 patterns optimize the structure and reduce parameter uncertainty of agent-based models (Grimm
644 et al. 2005).

645 The complexity of BOOSTIT, with 11 sub-models and almost 60 parameters, allowed a
646 satisfactory level of realism. It was important for us to represent many detailed processes to
647 answer the questions related to the boosted SIT for *B. dorsalis* in the Niayes area. We started
648 our modelling process by selecting some available empirical and expert knowledge. As the
649 development progressed, we added processes that were relevant to modelling goals. Our model
650 had become so complex with integrated knowledge that it could be considered a KIDS (Keep
651 It Descriptive, Stupid) model (Edmond sand Moss, 2005). However, the KIDS approach
652 proposes to start with a model that includes all variables and mechanisms that appear relevant
653 and then remove the ones that do not add to the quality of the model. In our case, we did not
654 use the validation patterns to remove processes as the KIDS approach proposes, mainly because
655 we wished BOOSTIT to be as generic as possible to be used in other contexts and scenarios.

656 BOOSTIT represents the spatial distribution of host trees and the related life-history events and
657 movements of flies with inter-individual interactions in lek areas and during reproduction. The
658 construction of the three types of landscapes allowed us to evidence variations of fly abundance
659 according to the quantity and carrying capacity of host fruits. To evaluate the success of SIT
660 and boosted SIT, we focused on the simple "monocultivar" landscape. Including landscape
661 heterogeneity in the model will serve to explore further the management techniques of *B.*
662 *dorsalis*, as was shown for the control of many other insect pests (e.g., Huang et al., 2017). We
663 also plan to explore the consequences of applying the SIT or boosted SIT in one or two orchards
664 instead of the four orchards of a landscape. For these two objectives, deeper explorations of the
665 SIT and boosted SIT will be conducted.

666 Our model validation based on comparisons with captured males (pheromone traps) in different
667 landscapes was the result of the interaction of several processes represented in BOOSTIT. We
668 used a visual method of comparison of our model dynamics with real-world data as adopted by

669 Yonow et al., (2004) and García Adeva and al., (2012) on capture data of *B. tryoni*, because we
670 were interested in the general pattern of the dynamic of fruit fly abundance. Yonow and al.,
671 (2004) and García Adeva and al., (2012) observed discrepancies between the predicted and
672 observed numbers of flies but their host plants phenological patterns used in their models were
673 approximately correct. This same situation was observed in the validation of our model, though
674 male capture data and the results of our simulation were expressed as a percentage of the
675 maximum to compare them. The decrease rate after the peak was slower in the simulation than
676 what was observed in the field. This could be explained by the effect of management methods
677 used in orchards and natural regulation by predators.

678 As noted in our simulation results, early population growth was linked to early maturing host
679 fruits. The first process explaining the landscape differences is the availability of the resource
680 for egg-laying. The earlier maturation dynamics of citrus compared to mango allowed
681 diversified landscapes to have early population growth. All our different mango cultivars had
682 the same initial carrying capacity, because little data on egg-laying preferences and larval
683 performance of *B. dorsalis* between mango cultivars were found. However, Diatta et al. (2013)
684 showed no differences of emerged adults per fruit between the Kent, Keitt and BDH cultivars.
685 The availability of resources was the main factor influencing the abundance of flies, with more
686 flies when many ripe fruits were available. Schwarzmueller and al. (2019) developed a
687 spatially-explicit model to predict the population dynamics of *B. tryoni.* They found that
688 abundance of *B. tryoni* was affected by resource compositions. In our model, differences in the
689 simulated landscapes are probably linked to these differences of fruit phenology and carrying
690 capacity.

691 The second process influencing fly phenology is the thermal dependency of the development,
692 survival and reproduction performances of *B. dorsalis*. We have a high degree of confidence in
693 our functions because this strong dependence on temperature was demonstrated in different
694 countries under laboratory conditions by Yang et al., (1994), Salum et al., (2014) and Dongmo
695 et al., (2021) and field conditions by Chen et Ye, (2007). The relative humidity was not
696 included. We have supposed that in our chosen orchards, humidity is favorable throughout the
697 year because of the irrigation systems used from March to August. These provide favorable
698 humidity for flies while waiting for the rainy season (de Villiers et al., 2015). The temperature
699 regime used in the presented simulation of BOOSTIT were obtained from the Niayes area. It
700 will be interesting in further work to explore how temperature regimes may influence
701 population dynamics in different latitudes.

The entomopathogen, *Metharizium anisopliae,* was represented in BOOSTIT as a number of spores that were introduced in the simulation by the sterile contaminated males and were transferred during flies' interactions. Each released sterile male had its spore number that decreased when it joined a lek and when it mated until it died. By representing the spores, we brought more realism to the *M. anisopliae* transfer. Unlike bacteria or virus- borned diseases, a fly contaminated with *M. anisopliae* does not contaminate other flies until it dies because if it survives a long time, it may not have enough spores to transfer the fatal dose to others. It was demonstrated that an inoculated fly could transfer the *M. anisopliae* to at least 3 mating lines of flies of the opposite sex before they died (Dimbi et al., 2013). This situation is reproduced by BOOSTIT: the mortality of contaminated sterile males being low during the first three days after their release, they actively transmit the pathogen. It was proven that *M. anisopliae* is pathogenic for *B. dorsalis* (Ekesi and al., 2011; Tora and Azerefegn, 2021). However, for modelling purposes, some lacking pieces of knowledge could have been very helpful. For example, we did not find any published data on the minimal spore dose of the entomopathogen that can kill the fly. Knowledge on the effects of temperature or relative humidity on the efficacy of the entomopathogen on flies in a natural environment would be very useful too. This information could provide more precision on our contamination process. By modifying the values of some parameters, BOOSTIT could also simulate outbreaks caused by other entomopathogenic fungi such as *Beauveria bassiana*.

Our results showed that both the boosted SIT and the SIT could reduce the population size of *B. dorsalis* with a better effect of boosted SIT. Models of Pleydell and Bouyer (2019) and Haramboure et al. (2020) also predict this result for a population of *Aedes* with the pyriproxyfen that targets the juvenile stage. In our model, *M. anisopliae* exerts its effect on the adult stage of the fly only, without any vertical transmission. Also, it was demonstrated on a grasshopper that when an insect dies from *M. anisopliae* contamination, this last emerges from the cadaver and sporulates if experiencing favorable climatic conditions (Arthurs et al., 2001). Thus, to improve the effectiveness of the boosted SIT on the reduction of the fly population, it would be interesting to see if the dead flies falling to the ground would be able to contaminate the pupas.

Pleydell and Bouyer (2019) and Haramboure et al. (2020) have considered different sterile male competitiveness and demonstrated that boosted SIT supported lower competitiveness of sterile males than the SIT. Unlike *Aedes albopictus*, *B. dorsalis* has a lek mating system where males participate in aggressive encounters with other males to defend sites from which to signal and court females. These in turn actively choose the most competitive males as partners (Hendrichs

et al., 2002). We know that laboratory-reared *B. dorsalis* can be fed with methyl-eugenol and be particularly competitive at lek time (Shelly, 1995; Orankanok et al., 2013). Thus, in our model, we assumed that sterile males are released with a high competitiveness level. This promotes boosted SIT and SIT and sterile males have a strong chance to transmit the entomopathogenic fungi. Further exploration of the model could consider to which level of competitiveness the sterile males could be reduced with still satisfactory results of the boosted SIT.

The SIT and the boosted SIT reduced and delayed the peak of fly population. Since the introduction of the Oriental fruit fly, mango producers harvest at an early maturity stage to avoid fruit fly infestation (Wangithi et al., 2021). In Senegal, the harvest period of the Kent cultivar generally lasts about one month. So, delay of 10 days allowed by the two control techniques is an important time saving to harvest non-stung fruits. The reduction of fly abundance with boosted SIT and SIT was not reflected in the same way on the number of stung fruits. This is a non-intuitive result. With fewer flies, one logically expects to have fewer damages. This suggests that looking at other aspects in addition to pest population size is very helpful to assess the success of the two control techniques. Most of the mathematical models assessed the success of the SIT by looking at the reduction of the population size only (Cai et al., 2014; Evans and Bishop, 2014). Some authors like Mishra et al. (2018) evaluated the success of the SIT on mosquitoes by looking at the disappearance or the persistence of the dengue fever. William et al. (2020) proposed control methods of SIT that allow reducing the mosquito population and the number of infected humans to the zika virus. It would be very useful to know from the models how much, for example, a 20% reduction in the fly population could reduce the amount of infested fruits. Such information could allow an optimization of the resources that are deployed for the management of the pest.

We chose an initial number of flies in our simulations to have enough of them surviving the period without available resources. This choice had been motivated by simulations with the "*intensive-landscape*" where there is no alternative host fruit before the Kent maturity stage. Another way to proceed could be to estimate the fly population density in the landscape by the mark-recapture method (Chailleux et al., 2021; Ito et al., 2021). The principle of this method consists of calculations based on the recapture of a percentage of marked and previously released insects. Despite not using this methodology, our model still succeeded in maintaining the fly population from year to year. The existence of this residual population shows that *B. dorsalis* can survive in the Niayes area of Senegal for a long time when climatic conditions are

not optimal and resources are not available. This is a new understanding of the invasion of this species in Senegal. It confirms previous studies (de Villiers et al., 2015; Magagula et al., 2015) that used two different programs (CLIMEX and MAXENT) to show the capacities of *B. dorsalis* to extend its distribution area despite sub-optimal conditions as long as irrigation is applied. It could be interesting to evaluate this in other places where *B. dorsalis* recently arrived.

To our knowledge, there are no data available on the predation rates of the fly. Thus, the fly mortality rate due to predation was not included. Some vertebrates (birds, bats, rodents) eat aborted fruits on the ground or ripe on the tree. In the process, they consume larvae contained in the fruits. Also, some insects such as weaver ants prey on larvae and pupae (Diame L. et al., 2015). The mortality of eggs and larvae due to larval competition has not been included in BOOSTIT unlike in the models of Yonow et al., (2004) and García Adeva et al., (2012). There is no consideration of a density-dependence because the information on larval density for the mango case in the Niayes area was not sufficient. However, we defined a carrying capacity for host plant patches, which makes that females could no longer lay eggs when the maximum carrying capacity was reached. Research on these different mortalities and the density dependence would be very useful to improve the model because they could reduce the fly population size. For the moment, BOOSTIT does not include other control methods of *B. dorsalis* like traps or orchard sanitation (Wangithi et al., 2021). Future developments could consider them in the context of studying the inclusion of boosted SIT in integrated pest management against *B. dorsalis*.

We have been able to use the available data to simulate the dynamics of the fly population in mango orchards, under releases of sterile males and sterile contaminated males. The overall degree of correspondence between the model results and the field data, and its ability to simulate SIT and boosted SIT scenarios suggest that the processes and parameters that drive the model are quite robust. Further research on some of the points described above would improve the model, as well as our understanding of the pathogen's transmission. Additionally, BOOSTIT can be adapted to other fruit flies or other climatic contexts. We expect BOOSTIT to become a useful tool to assist in the implementation of fruit fly management strategies.

Acknowledgements

This work was carried out with the financial support of a **L**ong-term **E**U- **A**frica research and innovation **P**artnership on food and nutrition security and sustainable **Agri**culture (LEAP-

Agri), project Pest-Free Fruit, in the framework of the European Union's Horizon 2020 research and innovation programme under grant agreement No 727715. It was also supported by the 2019 France-Senegal Research collaboration program of the French Embassy in Senegal and by CIRAD AI1. We wish to sincerely thank N.C. Manoukis and an anonymous reviewer whose comments greatly improved an earlier version of the manuscript.

References

Arthurs, S. p., Thomas, M. b., Lawton, J. l., 2001. Seasonal patterns of persistence and infectivity of *Metarhizium anisopliae* var. *acridum* in grasshopper cadavers in the Sahel. Entomol. Exp. Appl. 100, 69–76. https://doi.org/10.1046/j.1570-7458.2001.00849.x

Badii, K.B., Billah, M.K., Afreh Nuamah, K., Obeng Ofori, D., Nyarko, G., 2015. Review of the pest status, economic impact and management of fruit-infesting flies (Diptera: Tephritidae) in Africa. Afr. J. Agric. Res. 10, 1488–1498. https://doi.org/10.5897/AJAR2014.9278

Barclay, H.J., 1982. The sterile release method with unequal male competitive ability. Ecol. Model. 15, 251–263. https://doi.org/10.1016/0304-3800(82)90029-1

Barclay, H.J., McInnis, D., Hendrichs, J., 2014. Modeling the Area-Wide Integration of Male Annihilation and the Simultaneous Release of Methyl Eugenol-Exposed *Bactrocera spp*. Sterile Males. Ann. Entomol. Soc. Am. 107, 97–112. https://doi.org/10.1603/AN13010

Barclay, H.J., Vreysen, M.J.B., 2013. The interaction of dispersal and control methods for the riverine tsetse fly *Glossina palpalis gambiensis* (Diptera: Glossinidae): a modelling study. Popul. Ecol. 55, 53–68. https://doi.org/10.1007/s10144-012-0339-0

Barclay, H.J., Vreysen, M.J.B., 2011. A dynamic population model for tsetse (Diptera: Glossinidae) area-wide integrated pest management. Popul. Ecol. 53, 89–110. https://doi.org/10.1007/s10144-010-0224-7

Baumhover, A.H., Graham, A.J., Bitter, B.A., Hopkins, D.E., New, W.D., Dudley, F.H., Bushland, R.C., 1955. Screw-Worm Control Through Release of Sterilized Flies. J. Econ. Entomol. 48, 462–466. https://doi.org/10.1093/jee/48.4.462

Bouyer, J., Chandre, F., Gilles, J., Baldet, T., 2016. Alternative vector control methods to manage the Zika virus outbreak: more haste, less speed. Lancet Glob. Health 4, e364. https://doi.org/10.1016/S2214-109X(16)00082-6

Bouyer, J., Lefrançois, T., 2014. Boosting the sterile insect technique to control mosquitoes. Trends Parasitol. 30, 271–273. https://doi.org/10.1016/j.pt.2014.04.002

Cai, L., Ai, S., Li, J., 2014. Dynamics of Mosquitoes Populations with Different Strategies for Releasing Sterile Mosquitoes. SIAM J. Appl. Math. 74, 1786–1809. https://doi.org/10.1137/13094102X

Chailleux, A., Thiao, D.S., Diop, S., Bouvery, F., Ahmad, S., Caceres-Barrios, C., Faye, E., Brévault, T., Diatta, P., 2021. Understanding *Bactrocera dorsalis* trapping to calibrate area-wide management. J. Appl. Entomol. 145, 831–840. https://doi.org/10.1111/jen.12897

Chargui, Y., Dhahbi, A., Trabelsi, A., 2018. Extinction Conditions from a One-Sided Competition Model with a Holling Type I Functional Response for the Sterile Insect Technique. Open J. Model. Simul. 06, 13. https://doi.org/10.4236/ojmsi.2018.62002

Chen, P., Ye, H., 2007. Population dynamics of *Bactrocera dorsalis* (Diptera: Tephritidae) and analysis of factors influencing populations in Baoshanba, Yunnan, China. Entomol. Sci. 10, 141–147. https://doi.org/10.1111/j.1479-8298.2007.00208.x

Chinvinijkul, S., Limohpasmanee, W., Chanket, T., Uthaitanakit, A., Phopanit, P., Sukamnouyporn, W., Maneerat, C., Kimjong, W., Kumjing, P., Boonmee, N., 2019. Use of the Sterile Insect Technique in an Area-Wide Approach to Establish a Fruit Fly-Low Prevalence Area in Thailand, in: Area-Wide Management of Fruit Fly Pests. CRC Press.

Clarke, A., Amstrong, K.F., Carmichael, A.E., Milne, J.R., Roedrick, G.K., Yates, D.K., 2005. Invasive Phytophagous Pests Arising Through a Recent Tropical Evolutionary Raditation: THE *Bactrocera dorsalis* complex of fruit flies. Annu. Rev. Entomol. 50 293–319.

Danbaba, U.A., Garba, S.M., 2018. Modeling the transmission dynamics of Zika with sterile insect technique. Math. Methods Appl. Sci. 41, 8871–8896. https://doi.org/10.1002/mma.5336

de Villiers, M., Hattingh, V., Kriticos, D., Brunel, S., Vayssières, J.-F., Sinzogan, A.A.C., Billah, M., Mohamed, S., Mwatawala, M., Abdelgader, H., Salah, F.E.E., Meyer, M., 2015. The potential distribution of *Bactrocera dorsalis*: Considering phenology and irrigation patterns. Bull. Entomol. Res. 1, 1–15. https://doi.org/10.1017/S0007485315000693

Diame L., Rey J-Y., Sane C.A.B., Diatta P., Vayssieres J-F., Yasmine A., De Bon H., Grechi I., Diarra K., 2015. Influence of *Oecophylla longinoda* Latreille, 1802 (Hymenoptera : Formicidae) on mango infestation by *Bactrocera dorsalis* (Hendel) (Diptera : Tephritidae) in relation to Senegalese orchard design and management practices. Afr. Entomol. 23, 294–305. https://doi.org/10.10520/EJC176575

Diatta, P., Rey, J.-Y., Vayssieres, J.-F., Diarra, K., Coly, E.V., Lechaudel, M., Grechi, I., Ndiaye, S., Ndiaye, O., 2013. Fruit phenology of citruses, mangoes and papayas influences egg-laying preferences of *Bactrocera invadens* (Diptera: Tephritidae). Fruits 68, 507–516. https://doi.org/10.1051/fruits/2013093

Dimbi, S., Maniania, N., Ekesi, S., 2013. Horizontal Transmission of *Metarhizium anisopliae* in Fruit Flies and Effect of Fungal Infection on Egg Laying and Fertility. Insects 4, 206–216. https://doi.org/10.3390/insects4020206

Dimbi, S., Maniania, N.K., Ekesi, S., 2009. Effect of *Metarhizium anisopliae* inoculation on the mating behavior of three species of African Tephritid fruit flies, *Ceratitis capitata*, *Ceratitis cosyra* and *Ceratitis fasciventris*. Biol. Control 50, 111–116. https://doi.org/10.1016/j.biocontrol.2009.04.006

Dongmo, . Michel A., Fiaboe, K.K.M., Kekeunou, S., Nanga, S.N., Kuate, A.F., Tonnang, H.E.Z., Gnanvossou, D., Hanna, R., 2021. Temperature-based phenology model to predict the development, survival, and reproduction of the oriental fruit fly *Bactrocera dorsalis*. J. Therm. Biol. 97, 102877. https://doi.org/10.1016/j.jtherbio.2021.102877

Douchet, L., Haramboure, M., Baldet, T., L'Ambert, G., Damiens, D., Gouagna, L.C., Bouyer, J., Labbé, P., Tran, A., 2021. Comparing sterile male releases and other methods for integrated control of the tiger mosquito in temperate and tropical climates. Sci. Rep. 11, 7354. https://doi.org/10.1038/s41598-021-86798-8

Dufourd, C., Dumont, Y., 2013. Impact of environmental factors on mosquito dispersal in the prospect of sterile insect technique control. Comput. Math. Appl. 66, 1695–1715. https://doi.org/10.1016/j.camwa.2013.03.024

Dyck, V.A., Hendrichs, J., Robinson, A.S., 2021. Sterile Insect Technique : Principles And Practice In Area-Wide Integrated Pest Management. Taylor & Francis.

Edmonds, B., Moss, S., 2005. From KISS to KIDS – An 'Anti-simplistic' Modelling Approach, in: Davidsson, P., Logan, B., Takadama, K. (Eds.), Multi-Agent and Multi-Agent-Based Simulation, Lecture Notes in Computer Science. Springer Berlin Heidelberg, Berlin, Heidelberg, pp. 130–144. https://doi.org/10.1007/978-3-540-32243-6_11

Ekanayake, W.M.T.D., Jayasundara, M.S.H., Peek, T., Clarke, A.R., Schutze, M.K., 2017. The mating system of the true fruit fly *Bactrocera tryoni* and its sister species, *Bactrocera neohumeralis*. Insect Sci. 24, 478–490. https://doi.org/10.1111/1744-7917.12337

Ekesi, S., Maniania, N.K., Lux, S.A., 2002. Mortality in Three African Tephritid Fruit Fly Puparia and Adults Caused by the Entomopathogenic Fungi, *Metarhizium anisopliae* and *Beauveria bassiana.* Biocontrol Sci. Technol. 12, 7–17. https://doi.org/10.1080/09583150120093077

Ekesi, S., Maniania, N.K., Mohamed, S.A., 2011. Efficacy of soil application of *Metarhizium anisopliae* and the use of GF-120 spinosad bait spray for suppression of *Bactrocera invadens* (Diptera: Tephritidae) in mango orchards. Biocontrol Sci. Technol. 21, 299–316. https://doi.org/10.1080/09583157.2010.545871

Ekesi, S., Nderitu, P.W., Rwomushana, I., 2006. Field infestation, life history and demographic parameters of the fruit fly *Bactrocera invadens* (Diptera: Tephritidae) in Africa. Bull. Entomol. Res. 96, 379–386.

Enkerlin, W.R., 2021. Impact of fruit fly control programmes using the sterile insect technique, in: Dyck, V.A., Hendrichs, J., Robinson, A.S. (Eds.), Sterile Insect Technique Principles and Practice in Area-Wide Integrated Pest Management. pp. 979–1006.

Evans, T.P., Bishop, S.R., 2014. A spatial model with pulsed releases to compare strategies for the sterile insect technique applied to the mosquito *Aedes aegypti*. Math. Biosci. 254, 6–27. https://doi.org/10.1016/j.mbs.2014.06.001

Faye, E., Dangles, O., Pincebourde, S., 2016. Distance makes the difference in thermography for ecological studies. J. Therm. Biol. 56, 1–9. https://doi.org/10.1016/j.jtherbio.2015.11.011

Fister, K.R., McCarthy, M.L., Oppenheimer, S.F., 2018. Diffusing wild type and sterile mosquitoes in an optimal control setting. Math. Biosci. 302, 100–115. https://doi.org/10.1016/j.mbs.2018.05.015

Fister, K.R., McCarthy, M.L., Oppenheimer, S.F., Collins, C., 2013. Optimal control of insects through sterile insect release and habitat modification. Math. Biosci. 244, 201–212. https://doi.org/10.1016/j.mbs.2013.05.008

Fletcher, B.S., 1987. The biology of dacine fruit flies. Annu. Rev. Entomol. USA 32, 115–144.

Flores, S., Campos, S., Villaseñor, A., Valle, Á., Enkerlin, W., Toledo, J., Liedo, P., Montoya, P., 2013. Sterile males of *Ceratitis capitata* (Diptera: Tephritidae) as disseminators of *Beauveria bassiana* conidia for IPM strategies. Biocontrol Sci. Technol. 23, 1186–1198. https://doi.org/10.1080/09583157.2013.822473

García Adeva, J.J., Botha, J.H., Reynolds, M., 2012. A simulation modelling approach to forecast establishment and spread of *Bactrocera* fruit flies. Ecol. Model. 227, 93–108. https://doi.org/10.1016/j.ecolmodel.2011.11.026

Grechi, I., Preterre, A.-L., Caillat, A., Chiroleu, F., Ratnadass, A., 2021. Linking mango infestation by fruit flies to fruit maturity and fly pressure: A prerequisite to improve fruit fly damage management via harvest timing optimization. Crop Prot. 146, 105663. https://doi.org/10.1016/j.cropro.2021.105663

Grechi, I., Sane, C.A.B., Diame, L., Bon, H.D., Benneveau, A., Michels, T., Huguenin, V., Malezieux, E., Diarra, K., Rey, J.-Y., 2013. Mango-based orchards in Senegal: diversity of design and management patterns. Fruits 68, 447–466. https://doi.org/10.1051/fruits/2013094

Grimm, V., Berger, U., Bastiansen, F., Eliassen, S., Ginot, V., Giske, J., Goss-Custard, J., Grand, T., Heinz, S.K., Huse, G., Huth, A., Jepsen, J.U., Jørgensen, C., Mooij, W.M., Müller, B., Pe'er, G., Piou, C., Railsback, S.F., Robbins, A.M., Robbins, M.M., Rossmanith, E., Rüger, N., Strand, E., Souissi, S., Stillman, R.A., Vabø, R., Visser, U., DeAngelis, D.L., 2006. A standard protocol for describing individual-based and agent-based models. Ecol. Model. 198, 115–126. https://doi.org/10.1016/j.ecolmodel.2006.04.023

Grimm, V., Berger, U., DeAngelis, D.L., Polhill, J.G., Giske, J., Railsback, S.F., 2010. The ODD protocol: A review and first update. Ecol. Model. 221, 2760–2768. https://doi.org/10.1016/j.ecolmodel.2010.08.019

Grimm, V., Frank, K., Jeltsch, F., Brandl, R., Uchmański, J., Wissel, C., 1996. Pattern-oriented modelling in population ecology. Sci. Total Environ., Modelling in Environmental Studies 183, 151–166. https://doi.org/10.1016/0048-9697(95)04966-5

Grimm, V., Railsback, S.F., 2013. Individual-based Modeling and Ecology, Individual-based Modeling and Ecology. Princeton University Press.

Grimm, V., Railsback, S.F., 2006. Agent-Based Models in Ecology: Patterns and Alternative Theories of Adaptive Behaviour, in: Billari, F.C., Fent, T., Prskawetz, A., Scheffran, J. (Eds.), Agent-Based Computational Modelling: Applications in Demography, Social, Economic and Environmental Sciences, Contributions to Economics. Physica-Verlag HD, Heidelberg, pp. 139–152. https://doi.org/10.1007/3-7908-1721-X_7

Grimm, V., Railsback, S.F., Vincenot, C.E., Gallagher, C., DeAngelis, D.L., Edmonds, B., Ge, J., Giske, J., Groeneveld, J., Johnston, A.S.A., Milles, A., Nabe-Nielsen, J., Polhill, J.G., 2020. The ODD Protocol for Describing Agent-Based and Other Simulation Models: A Second Update to Improve Clarity, Replication, and Structural Realism 20.

Grimm, V., Revilla, E., Berger, U., Jeltsch, F., Mooij, W.M., 2005. Pattern-Oriented Modeling of Agent-Based Complex Systems: Lessons from Ecology. Science 310, 987–991. https://doi.org/10.1126/science.1116681

Gutierrez, A.P., Ponti, L., Neteler, M., Suckling, D.M., Cure, J.R., 2021. Invasive potential of tropical fruit flies in temperate regions under climate change. Commun. Biol. 4, 1–14. https://doi.org/10.1038/s42003-021-02599-9

Haramboure, M., Labbé, P., Baldet, T., Damiens, D., Gouagna, L.C., Bouyer, J., Tran, A., 2020. Modelling the control of *Aedes albopictus* mosquitoes based on sterile males release techniques in a tropical environment. Ecol. Model. 424, 109002. https://doi.org/10.1016/j.ecolmodel.2020.109002

Hendrichs, J., Pereira, R., Vreysen, M.J.B., 2020. Area-Wide Integrated Pest Management: Development and Field Application. CRC Press.

Hendrichs, J., Robinson, A.S., Cayol, J.P., Enkerlin, W., 2002. Medfly areawide sterile insect technique programmes for prevention, suppression or eradication: the importance of mating behavior studies. Fla. Entomol. 85, 1–13. https://doi.org/10.1653/0015-4040(2002)085[0001:MASITP]2.0.CO;2

Hokkanen, H., Menzler-Hokkanen, I., 2007. Use of honeybees in the biological control of plant diseases, in: Unknown Host Publication. Presented at the International Congress of Insect Biotechnology & Industry (ICIBI), pp. A62–A63.

Huang, M., Song, X., Li, J., 2017. Modelling and analysis of impulsive releases of sterile mosquitoes. J. Biol. Dyn. 11, 147–171. https://doi.org/10.1080/17513758.2016.1254286

Ito, Y., Yamamura, K., Manoukis, N.C., 2021. Role of population and behavioural ecology in the sterile insect technique, in: Dyck, V.A., Hendrichs, J., Robinson, A.S. (Eds.), Sterile Insect Technique Principles and Practice in Area-Wide Integrated Pest Management. pp. 245–282.

Kean, J.M., Maxwell Suckling, D., Stringer, L.D., Woods, B., 2011. Modeling the Sterile Insect Technique for Suppression of Light Brown Apple Moth (Lepidoptera: Tortricidae). J. Econ. Entomol. 104, 1462–1475. https://doi.org/10.1603/EC11086

Klassen, W., Curtis, C.F., Hendrichs, J., 2021. History of the sterile insect technique, in: Dyck, V.A., Hendrichs, J., Robinson, A.S. (Eds.), Sterile Insect Technique. Principles and Practice in Area-Wide Integrated Pest Management. pp. 1–45.

Lance, D.R., McInnis, D.O., 2021. Biological basis of the sterile insect technique, in: Dyck, V.A., Hendrichs, J., Robinson, A.S. (Eds.), Sterile Insect Technique: Principles and Practice in Area-Wide Integrated Pest Management. pp. 113–142.

Liang, J., Yan, Q., Xiang, C., Tang, S., 2019. A reaction-diffusion population growth equation with multiple pulse perturbations. Commun. Nonlinear Sci. Numer. Simul. 74, 122–137. https://doi.org/10.1016/j.cnsns.2019.02.015

Liu, J.-H., Xiong, X., Pan, Y., Xiong, Z., Deng, Z., Yang, L., 2011. Predicting potential distribution of oriental fruit fly, *Bactrocera dorsalis* in Jiangxi Province, South China based on maximum entropy model. Sci Res Essays 7.

Lux, S., Copeland, R., White, I., Manrakhan, A., Billah, M., 2003. A New Invasive Fruit Fly Species from the *Bactrocera dorsalis* (Hendel) Group Detected in East Africa. Int. J. Trop. Insect Sci. 23, 355–361. https://doi.org/10.1017/S174275840001242X

Magagula, C.N., Cugala, D.C., Monadjem, A., Dlamini, W.M., 2015. Predicted Regional and National Distribution of *Bactrocera dorsalis* (syn. B. invadens) (Diptera: Tephritidae) in Southern Africa and Implications for Its Management. Afr. Entomol. 23, 427–437. https://doi.org/10.4001/003.023.0220

Manoukis, N.C., Colliers, T.C., 2021. Agent-Based Simulations to Determine Mediterranean Fruit Fly Declaration of Eradication Following Outbreaks: Concepts and Practical Examples, in: Hendrichs, J., Pereira, R., Vreysen, M.J.B. (Eds.), Area-Wide Integrated Pest Management Development and Field Application. CRC Press, pp. 868–888. https://doi.org/10.1201/9781003169239-50

Manoukis, N.C., Hoffman, K., 2014. An agent-based simulation of extirpation of *Ceratitis capitata* applied to invasions in California. J. Pest Sci. 87, 39–51. https://doi.org/10.1007/s10340-013-0513-y

Manrakhan, A., Venter, J.H., Hattingh, V., 2015. The progressive invasion of *Bactrocera dorsalis* (Diptera: Tephritidae) in South Africa. Biol. Invasions 17, 2803–2809. https://doi.org/10.1007/s10530-015-0923-2

Mishra, A., Ambrosio, B., Gakkhar, S., Aziz-Alaoui, M.A., 2018. A Network Model for Control of Dengue Epidemic Using Sterile Insect Technique. Math. Biosci. Eng. 15, 441–460. https://doi.org/10.3934/mbe.2018020

Multerer, L., Smith, T., Chitnis, N., 2019. Modeling the impact of sterile males on an *Aedes aegypti* population with optimal control. Math. Biosci. 311, 91–102. https://doi.org/10.1016/j.mbs.2019.03.003

Mwatawala, M.W., Mziray, H., Malebo, H., De Meyer, M., 2015. Guiding farmers' choice for an integrated pest management program against the invasive *Bactrocera dorsalis* (Hendel) (Diptera: Tephritidae) in mango orchards in Tanzania. Crop Prot. 76, 103–107. https://doi.org/10.1016/j.cropro.2015.07.001

Novelo-Rincón, L.F., Montoya, P., Hernández-Ortíz, V., Liedo, P., Toledo, J., 2009. Mating performance of sterile Mexican fruit fly *Anastrepha ludens* (Dipt., Tephritidae) males used as vectors of *Beauveria bassiana* (Bals.) Vuill - Novelo-Rincón - 2009 - Journal of Applied Entomology - Wiley Online Library [www Document]. URL https://onlinelibrary.wiley.com/doi/epdf/10.1111/j.1439-0418.2009.01427.x (accessed 3.25.20).

Onsongo, S.K., Gichimu, B.M., Akutse, K.S., Dubois, T., Mohamed, S.A., 2019. Performance of Three Isolates of *Metarhizium anisopliae* and Their Virulence against *Zeugodacus cucurbitae* under Different Temperature Regimes, with Global Extrapolation of Their Efficiency. Insects 10, 270.

Orankanok, W., Chinvinijkul, S., Sawatwangkhoung, A., Pinkaew, S., Orankanok, S., 2013. Methyl eugenol and pre-release diet improve mating performance of young *Bactrocera dorsalis* and *Bactrocera correcta* males. J. Appl. Entomol. 137, 200–209. https://doi.org/10.1111/j.1439-0418.2011.01677.x

Orankanok, W., Chinvinijkul, S., Thanaphum, S., Sitilob, P., Enkerlin, W.R., 2007. Area-Wide Integrated Control of Oriental Fruit Fly *Bactrocera dorsalis* and Guava Fruit Fly *Bactrocera correcta* in Thailand. Springer Netherlands, pp. 517–526. https://doi.org/10.1007/978-1-4020-6059-5_48

Ouna, E.A., Birgen, J., Ekesi, S., 2010. Entomopathogenicity of hyphomycete fungi to fruit fly *Bactrocera invadens* (Diptera Tephritidae) and their potential for biological control on mango.

Piou, C., Prévost, E., 2012. A demo-genetic individual-based model for Atlantic salmon populations: Model structure, parameterization and sensitivity. Ecol. Model. 231, 37–52. https://doi.org/10.1016/j.ecolmodel.2012.01.025

Pleydell, D.R.J., Bouyer, J., 2019. Biopesticides improve efficiency of the sterile insect technique for controlling mosquito-driven dengue epidemics. Commun. Biol. 2, 1–11. https://doi.org/10.1038/s42003-019-0451-1

Potgieter, L., van Vuuren, J.H., Conlong, D.E., 2013. A reaction–diffusion model for the control of *Eldana saccharina* Walker in sugarcane using the sterile insect technique. Ecol. Model. 250, 319–328. https://doi.org/10.1016/j.ecolmodel.2012.11.019

Potgieter, L., Vuuren, J. van, Conlong, D.E., 2012. Modelling the effects of the sterile insect technique applied to *Eldana saccharina* Walker in sugarcane. ORiON 28, 59–84.

Qin, Y., Wang, C., Zhao, Z., Pan, X., Li, Z., 2019. Climate change impacts on the global potential geographical distribution of the agricultural invasive pest, *Bactrocera dorsalis* (Hendel) (Diptera: Tephritidae). Clim. Change 155, 145–156. https://doi.org/10.1007/s10584-019-02460-3

Quesada-Moraga, E., Martin-Carballo, I., Garrido-Jurado, I., Santiago-Álvarez, C., 2008. Horizontal transmission of *Metarhizium anisopliae* among laboratory populations of *Ceratitis capitata* (Wiedemann) (Diptera: Tephritidae). Biol. Control 47, 115–124. https://doi.org/10.1016/j.biocontrol.2008.07.002

Quesada-Moraga, E., Ruiz-García, A., Santiago-Álvarez, C., 2006. Laboratory Evaluation of Entomopathogenic Fungi *Beauveria bassiana* and *Metarhizium anisopliae* Against Puparia and Adults of *Ceratitis capitata* (Diptera: Tephritidae). J. Econ. Entomol. 99, 1955–1966. https://doi.org/10.1093/jee/99.6.1955

Ramirez, S., Gordillo, L.F., 2016. Approximating Optimal Release in a Deterministic Model for the Sterile Insect Technique. Int. J. Agron. 2016, e8492107. https://doi.org/10.1155/2016/8492107

Rodríguez, N., 2015. On an integro-differential model for pest control in a heterogeneous environment. J. Math. Biol. 70, 1177–1206. https://doi.org/10.1007/s00285-014-0793-8

Rwomushana, I., Ekesi, S., Gordon, I., Ogol, C.K.P.O., 2008. Host Plants and Host Plant Preference Studies for *Bactrocera invadens* (Diptera: Tephritidae) in Kenya, a New Invasive Fruit Fly Species in Africa. Ann. Entomol. Soc. Am. 101, 331–340. https://doi.org/10.1603/0013-8746(2008)101[331:HPAHPP]2.0.CO;2

Salum, J.K., Mwatawala, M.W., Kusolwa, P.M., Meyer, M.D., 2014. Demographic parameters of the two main fruit fly (Diptera: Tephritidae) species attacking mango in Central Tanzania. J. Appl. Entomol. 138, 441–448. https://doi.org/10.1111/jen.12044

Sarron, J., Malézieux, É., Sané, C.A.B., Faye, É., 2018. Mango Yield Mapping at the Orchard Scale Based on Tree Structure and Land Cover Assessed by UAV. Remote Sens. 10, 1900. https://doi.org/10.3390/rs10121900

Schutze, M.K., Aketarawong, N., Amornsak, W., Armstrong, K.F., Augustinos, A.A., Barr, N., Bo, W., Bourtzis, K., Boykin, L.M., Cáceres, C., Cameron, S.L., Chapman, T.A., Chinvinijkul, S., Chomič, A., De Meyer, M., Drosopoulou, E., Englezou, A., Ekesi, S., Gariou-Papalexiou, A., Geib, S.M., Hailstones, D., Hasanuzzaman, M., Haymer, D., Hee, A.K.W., Hendrichs, J., Jessup, A., Ji, Q., Khamis, F.M., Krosch, M.N., Leblanc, L., Mahmood, K., Malacrida, A.R., Mavragani-Tsipidou, P., Mwatawala, M., Nishida, R., Ono, H., Reyes, J., Rubinoff, D., San Jose, M., Shelly, T.E., Srikachar, S., Tan, K.H., Thanaphum, S., Haq, I., Vijaysegaran, S., Wee, S.L., Yesmin, F., Zacharopoulou, A., Clarke, A.R., 2015. Synonymization of key pest species within the *Bactrocera dorsalis* species complex (Diptera: Tephritidae): taxonomic changes based on a review of 20 years of integrative morphological, molecular, cytogenetic, behavioural and chemoecological data. Syst. Entomol. 40, 456–471. https://doi.org/10.1111/syen.12113

Schwarzmueller, F., Schellhorn, N.A., Parry, H., 2019. Resource landscapes and movement strategy shape Queensland Fruit Fly population dynamics. Landsc. Ecol. 34, 2807–2822. https://doi.org/10.1007/s10980-019-00910-y

Shelly, T.E., 2000. Fecundity of Female Oriental Fruit Flies (Diptera: Tephritidae): Effects of Methyl Eugenol-Fed and Multiple Mates. Ann. Entomol. Soc. Am. 93, 559–564. https://doi.org/10.1603/0013-8746(2000)093[0559:FOFOFF]2.0.CO;2

Shelly, T.E., 1995. Methyl Eugenol and the Mating Competitiveness of Irradiated Male *Bactrocera dorsalis* (Diptera: Tephritidae). Ann. Entomol. Soc. Am. 88, 883–886. https://doi.org/10.1093/aesa/88.6.883

Sookar, P., Bhagwant, S., Allymamod, M.N., 2014. Effect of *Metarhizium anisopliae* on the fertility and fecundity of two species of fruit flies and horizontal transmission of mycotic infection. J. Insect Sci. 14, 12.

Stephens, A.E.A., Kriticos, D.J., Leriche, A., 2007. The current and future potential geographical distribution of the oriental fruit fly, *Bactrocera dorsalis* (Diptera: Tephritidae). Bull. Entomol. Res. 97, 369. https://doi.org/10.1017/S0007485307005044

Strugarek, M., 2019. On the use of the sterile insect release technique to reduce or eliminate mosquito populations. Appl. Math. Model. 28.

Sutantawong, M., Orankanok, W., Enkerlin, W.R., Wornoayporn, V., Caceres, C., 2002. The sterile insect technique for control of the oriental fruit fly, *Bactrocera dorsalis* (Hendel), in mango orchards in Ratchaburi Province, Thailand 10.

Thomé, R.C.A., Yang, H.M., Esteva, L., 2010. Optimal control of Aedes aegypti mosquitoes by the sterile insect technique and insecticide. Math. Biosci. 223, 12–23. https://doi.org/10.1016/j.mbs.2009.08.009

Tora, M., Azerefegn, F., 2021. Virulence of *Beauveria bassiana* and *Metarhizium anisopliae* Isolates against the Oriental Fruit Fly Bactrocera dorsalis (Diptera: Tephritidae) Hendel under Laboratory Conditions. Ethiop. J. Agric. Sci. 31, 53–67.

Tyson, R., Thistlewood, H., Judd, G.J.R., 2007. Modelling dispersal of sterile male codling moths, *Cydia pomonella*, across orchard boundaries. Ecol. Model. 205, 1–12. https://doi.org/10.1016/j.ecolmodel.2006.12.038

Vreysen, M.J.B., Barclay, H.J., Hendrichs, J., 2006. Modeling of Preferential Mating in Areawide Control Programs That Integrate the Release of Strains of Sterile Males Only or Both Sexes. Ann. Entomol. Soc. Am. 99, 607–616. https://doi.org/10.1603/0013-8746(2006)99[607:MOPMIA]2.0.CO;2

Wangithi, C.M., Muriithi, B.W., Belmin, R., 2021. Adoption and Dis-Adoption of Sustainable Agriculture: A Case of Farmers' Innovations and Integrated Fruit Fly Management in Kenya. Agriculture 11, 338. https://doi.org/10.3390/agriculture11040338

Wei, D., Feng, Y.-C., Wei, D.-D., Yuan, G.-R., Dou, W., Wang, J.-J., 2015. Female remating inhibition and fitness of *Bactrocera dorsalis* (Diptera: Tephritidae) associated with male accessory glands. Fla. Entomol. 98, 52–58. https://doi.org/10.1653/024.098.0110

Wiegand, T., Jeltsch, F., Hanski, I., Grimm, V., 2003. Using pattern-oriented modeling for revealing hidden information: a key for reconciling ecological theory and application. Oikos 100, 209–222. https://doi.org/10.1034/j.1600-0706.2003.12027.x

Wiegand, T., Naves, J., Stephan, T., Fernandez, A., 1998. Assessing the Risk of Extinction for the Brown Bear (ursus Arctos) in the Cordillera Cantabrica, Spain. Ecol. Monogr. 68, 539–570. https://doi.org/10.1890/0012-9615(1998)068[0539:ATROEF]2.0.CO;2

William, A., Johnson, A., Alih, D.M., Samuel, O.K., Godwin, C.E.M., 2020. Modeling the Impact of Optimal Control Strategies on the Dynamics of Zika Virus Disease Using the Sterile Insect Technology. J. Adv. Math. Comput. Sci. 13–33. https://doi.org/10.9734/jamcs/2020/v35i830310

Yang, C., Zhang, X., Li, J., 2020. Dynamics of two-patch mosquito population models with sterile mosquitoes. J. Math. Anal. Appl. 483, 123660. https://doi.org/10.1016/j.jmaa.2019.123660

Yang et al., n.d. Temperature Influences on the Development and Demography of *Bactrocera dorsalis* (Diptera: Tephritidae) in China.

Yang, P., Carey, J.R., Dowell, R.V., 1994. Temperature Influences on the Development and Demography of *Bactrocera dorsalis* (Diptera: Tephritidae) in China. Physiol. Chem. Ecol. 23, 971–974.

Yonow, T., Zalucki, M.P., Sutherst, R.W., Dominiak, B.C., Maywald, G.F., Maelzer, D.A., Kriticos, D.J., 2004. Modelling the population dynamics of the Queensland fruit fly, *Bactrocera* (Dacus) *tryoni*: a cohort-based approach incorporating the effects of weather. Ecol. Model. 173, 9–30. https://doi.org/10.1016/S0304-3800(03)00306-5

Yousef, M., Garrido-Jurado, I., Ruíz-Torres, M., Quesada-Moraga, E., 2017. Reduction of adult olive fruit fly populations by targeting preimaginals in the soil with the entomopathogenic fungus *Metarhizium brunneum*. J. Pest Sci. 90, 345–354. https://doi.org/10.1007/s10340-016-0779-y

Zimmermann, G., 2007. Review on safety of the entomopathogenic fungus *Metarhizium anisopliae*. Biocontrol Sci. Technol. 17, 879–920. https://doi.org/10.1080/09583150701593963

Appendix

Appendix A: development of immature stages of *B. dorsalis* according to temperature (García Adeva et al., 2012)

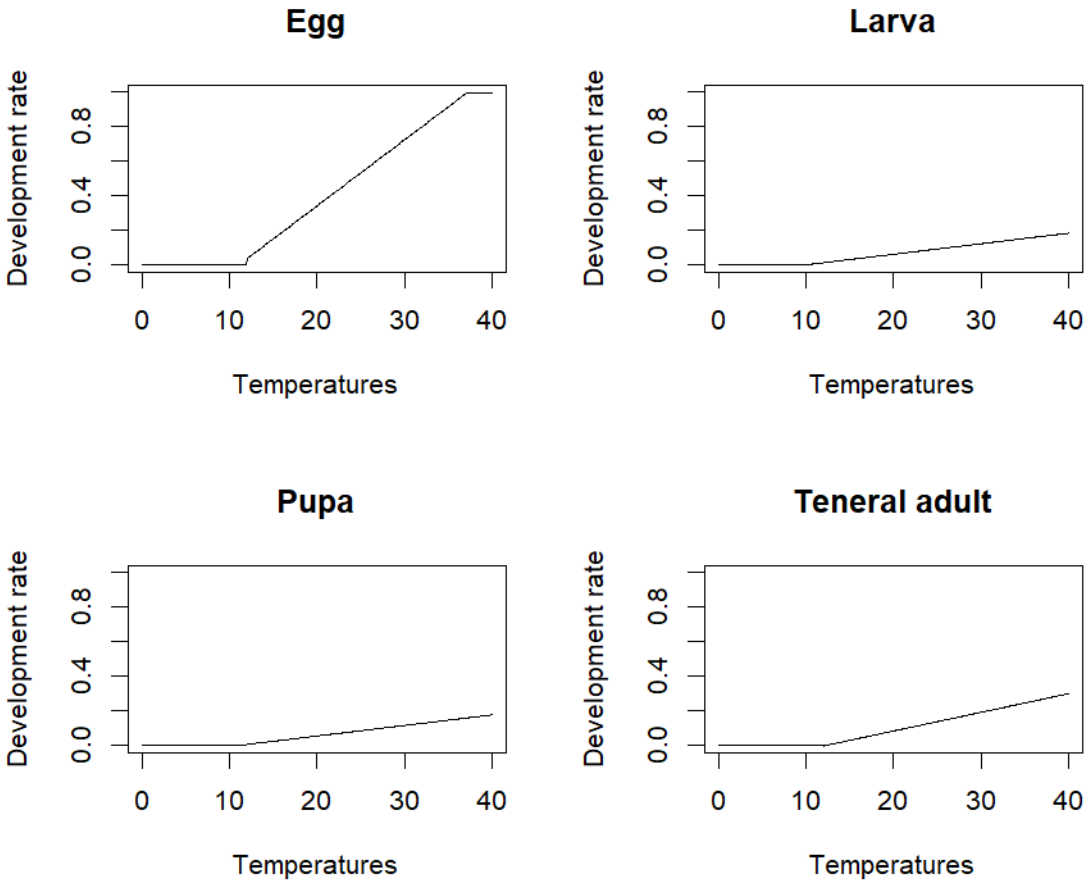

Appendix B: Mortality of different stages of *B. dorsalis* according to temperature (Yang et al., 1994; Yonow et al., 2004; García Adeva et al., 2012)

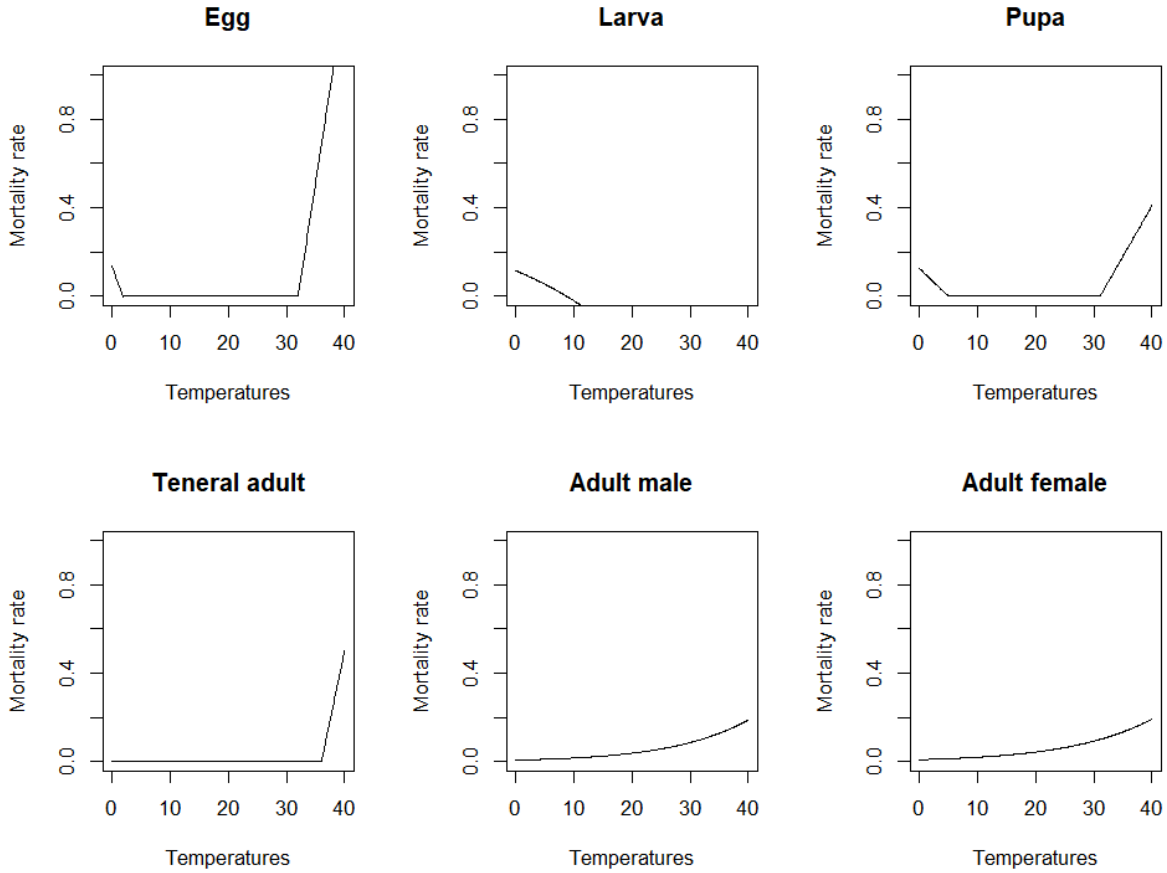

Appendix C: Pre-oviposition period of female *B. dorsalis* according to temperature (Yang et al., 1994)

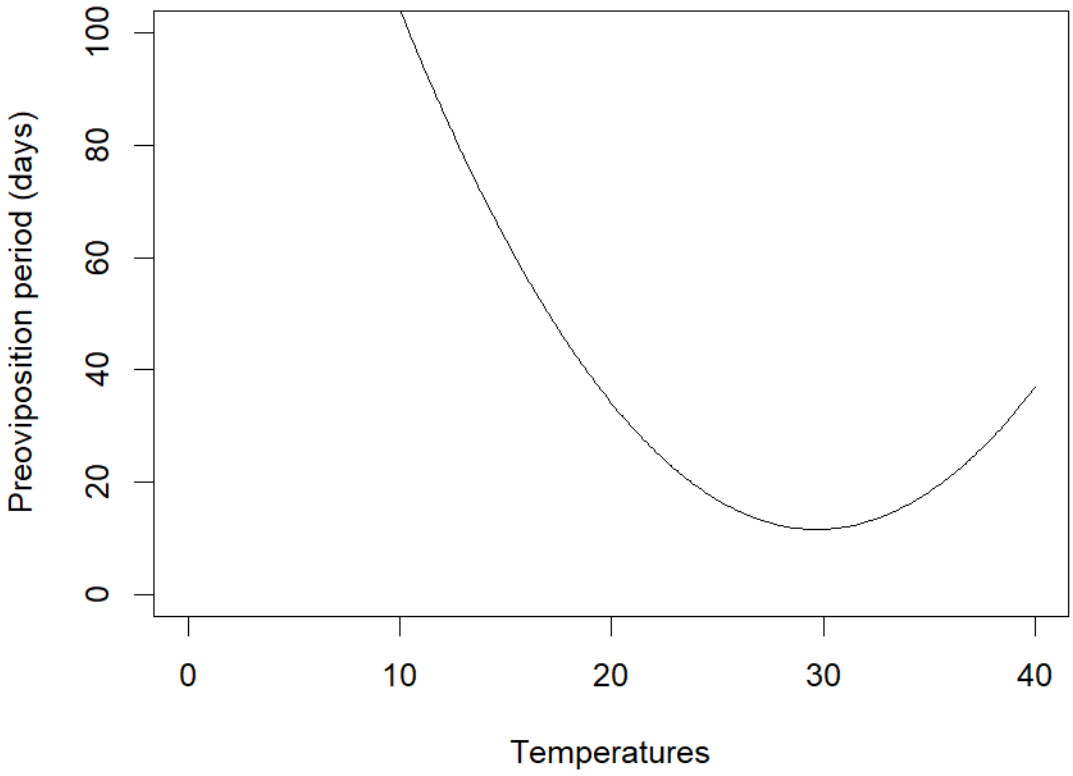

1171 **Appendix D**: Egg number laid by female *B. dorsalis* according to temperature (Yang et al., 1994)

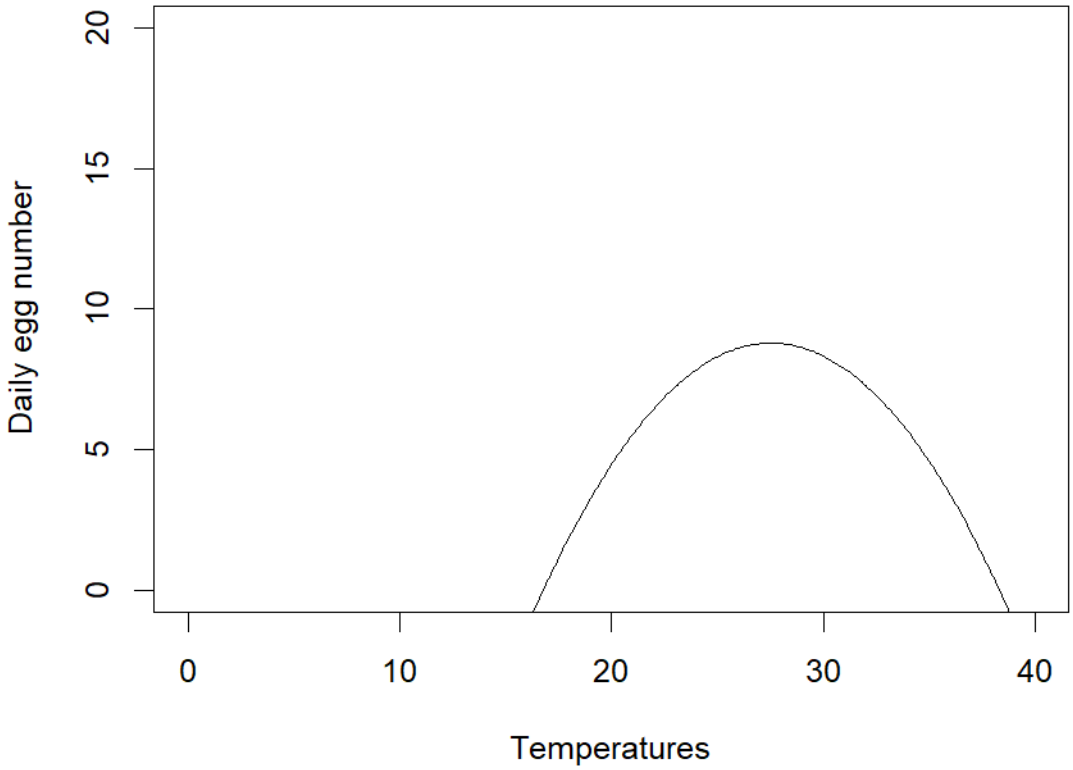

1172